POWER REACTOR TECHNOLOGY

A Quarterly Technical Progress Review

Prepared for DIVISION OF TECHNICAL INFORMATION, USAEC, by
W. H. ZINN and J. R. DIETRICH, COMBUSTION ENGINEERING, INC., NUCLEAR DIVISION

Spring 1965

● VOLUME 8

● NUMBER 2

TECHNICAL PROGRESS REVIEWS

To meet the needs of industry for concise summaries of current atomic developments, the Atomic Energy Commission is publishing this series, Technical Progress Reviews. Issued quarterly, each of the reviews digests and evaluates the latest findings in a specific area of nuclear technology and science.

The five journals published in this series are:

Isotopes and Radiation Technology, P. S. Baker, A. F. Rupp, and associates, Oak Ridge National Laboratory

Nuclear Safety, Wm. B. Cottrell, W. H. Jordan, and associates, Oak Ridge National Laboratory

Power Reactor Technology, W. H. Zinn and J. R. Dietrich, Combustion Engineering, Inc., Nuclear Division

Reactor Fuel Processing, Stephen Lawroski and associates, Chemical Engineering Division, Argonne National Laboratory

Reactor Materials, R. W. Dayton, E. M. Simons, and associates, Battelle Memorial Institute

Each journal may be purchased from the Superintendent of Documents, U. S. Government Printing Office, Washington, D. C., 20402. *Isotopes and Radiation Technology* at $2.00 per year for subscription or $0.55 for individual issues; the other four journals at $2.50 per year and $0.70 per issue. See back cover for remittance instructions and foreign postage requirements.

Availability of Reports Cited in This Review

Unclassified AEC reports are available for inspection at AEC depository libraries and are sold by the Clearinghouse for Federal Scientific and Technical Information, National Bureau of Standards, U. S. Department of Commerce, 5285 Port Royal Road, Springfield, Va., 22151. Some of the reports cited are not available owing to their preliminary nature; however, the information contained in them will eventually be made available in formal progress or topical reports.

Unclassified reports issued by other Government agencies or private organizations should be requested from the originator.

Unclassified British and Canadian reports may be inspected at AEC depository libraries. British reports are sold by the British Information Service, 45 Rockefeller Plaza, New York, N. Y.; Canadian reports (AECL series) are sold by the Scientific Document Distribution Office, Atomic Energy of Canada, Ltd., Chalk River, Ontario, Canada.

Classified U. S. and foreign reports identified in this journal as Classified may be purchased by properly cleared Access Permit Holders from the Division of Technical Information Extension, U. S. Atomic Energy Commission, P. O. Box 1001, Oak Ridge, Tenn., 37831. Such reports may be inspected at classified AEC depository libraries.

POWER REACTOR TECHNOLOGY

A REVIEW OF RECENT DEVELOPMENTS

Prepared for DIVISION OF TECHNICAL INFORMATION, USAEC,
by W. H. ZINN and J. R. DIETRICH,
COMBUSTION ENGINEERING, INC., NUCLEAR DIVISION

SPRING 1965

VOLUME 8

NUMBER 2

Foreword

This quarterly review of reactor development has been prepared at the request of the Division of Technical Information of the U. S. Atomic Energy Commission. Its purpose is to assist interested organizations in the task of keeping abreast of new results in reactor technology for civilian application.

Power Reactor Technology contains reviews of selected recently published reports that are judged noteworthy in the fields of power-reactor research and development, power-reactor applications, design practice, and operating experience. It is not meant to be a comprehensive abstract of all material published during the quarter, nor is it meant to be a treatise on any part of the subject. However, related reports from different sources are often treated together to yield reviews having some breadth of scope, and background material may be added to place recent developments in perspective. Occasionally the reviews are written by guest authors. Reviews having unusual breadth or significance are placed at the front of the issue as Feature Articles.

The intention is to cover the various areas of reactor development from the general viewpoint of the reactor designer rather than from the more detailed points of view of specialists in the individual areas. To whatever extent the coverage of *Power Reactor Technology* may occasionally overlap the fields of the other Technical Progress Reviews, the overlaps will be motivated by this objective of viewing current progress through the eyes of the reactor designer.

A degree of critical appraisal and some interpretation of results are often necessary to define the significance of reported work. Any such appraisal or interpretation represents only the opinion of the reviewer and (in the usual case, when the review is written by Combustion Engineering, Inc., Nuclear Division staff) the Editor. When the review is predominantly interpretive the reviewer is named; unless identified as a guest author, he is a member of the Combustion Engineering, Inc., Nuclear Division staff. Readers are urged to consult the original references to obtain all the background of the work reported and to obtain the interpretation of the results given by the original authors.

For timely coverage, *Power Reactor Technology* must often review fragmentary material. The fixed subject headings listed below have been adopted in the hope of maintaining some continuity and order in the material from one issue to another: all reviews except Feature Articles will be arranged under these headings. A particular issue will not necessarily contain all the headings but only those under which material is reviewed.

Economics, Applications, Programs
Resources and Fuel Cycles
Physics
Fluid and Thermal Technology
Fuel Elements
Materials
Control and Dynamics
Containment, Radiation Control, and Siting
Systems Technology
Components
Design and Construction Practice
Operating Experience
Specific Reactor Types
Specific Applications
Unconventional Approaches

W. H. Zinn, Vice-President
J. R. Dietrich, Editor
Combustion Engineering, Inc.

Contents

Issued quarterly by the U. S. Atomic Energy Commission. Use of funds for printing this publication approved by the Director of the Bureau of the Budget on October 14, 1963.

Letter to the Editor

WESTINGHOUSE ATOMIC POWER DIVISION
EXPERIENCE WITH STAINLESS-STEEL-CLAD FUEL ELEMENTS

In marked contrast to the VBWR results reported in *Power Reactor Technology*, 7, 4, Westinghouse has not observed failure of stainless steel cladding in a pressurized water reactor environment. Our operating experience to date is summarized in Table I. Stainless steel has clearly performed with distinction under exposures substantially in excess of those at which failures occurred in VBWR, regardless of whether the cladding was annealed or cold worked, freestanding or collapsed. Yankee environment was primary neutral, with periods of high *p*H and boric acid operation; Saxton and Selni are chemical shim systems (boric acid) having added alkali.

Table I IRRADIATION DATA ON STAINLESS-STEEL FUEL ELEMENTS IN WESTINGHOUSE REACTORS

Stainless type	Cladding thickness, in.	Peak exposure		Reactor
		Nvt >1 Mev	MWD/MTU	
Annealed 348	0.021 (freestanding)	7×10^{21}	30,000	Yankee
Cold worked 304	0.016 (freestanding)	3×10^{21}	20,300	Saxton
Cold worked 304	0.010 (collapsed)	1×10^{21}	10,000	Saxton
Cold worked 304	0.015 (freestanding)	1×10^{21}	6,000	Selni

A test assembly irradiated in Yankee Cores I and II is now under test in Core IV and will achieve a peak burnup of 41,000 MWD/MTU (fast flux >1 Mev = 11×10^{21} nvt) by September 1965. Fuel elements in the basic Saxton Core will achieve peak exposures of 25,000 MWD/MTU by June 1965. Selni fuel elements will achieve 16,000 MWD/MTU by July 1966.

Based on an extensive review of experimental data reported by other laboratories, we conclude that in-reactor failures of UO_2 fuel elements clad with commercial stainless steel have occurred only in a boiling water environment. Factors which must be evaluated in explaining the differences between stainless steel behavior in boiling and pressurized water reactors are as follows:

1. *System Pressure*

The higher system pressure in a pressurized water reactor produces a larger compressive stress component on the cladding surface. For example, the circumferential compressive stress contribution from 2,000 psi external pressure will be about 12,000 psi greater than in a boiling water system operating at 1,000 psi, assuming equivalent clad thickness and geometry. The higher system pressure thus prevents or delays the development of tensile stress in the cladding as a result of fission gas accumulation. Crack propagation cannot normally occur in the absence of a tensile stress.

2. *System Chemistry*

Typically, oxygen concentration in pressurized water is less than 0.01 ppm. In direct cyclic boiling systems, however, oxygen in the vapor stage varies from 20–40 ppm; in the liquid, oxygen concentration is typically 0.05 to 0.5 ppm. High oxygen concentrations have been shown in laboratory experiments to accelerate stress corrosion. Differences in corrosion behavior may also arise from differences in the equilibrium distribution of chemical species from radiolytic decomposition.

3. *Corrosion Product Deposition*

Corrosion products deposit on the surfaces of fuel elements irradiated in both boiling and nonboiling water environment (although the examination of the irradiated Yankee elements revealed almost no deposited corrosion product). The corrosion product deposited from a boiling coolant will be highly oxidized; ferric ions are known to be effective crack promoters.

4. *Local Thermal Stresses*

Fundamental heat transfer studies[1,2,3] have shown that rapid thermal fluctuations occur at surfaces where boiling is occurring. These local temperature fluctuations are caused by the growth and detachment of vapor bubbles which temporarily change the local heat transfer rates at the fuel element surface. Amplitude of the observed temperature variations ranges from a few degrees to about 30°F, occurring at somewhat irregular intervals of 3–50 milliseconds. The rate at which the temperature decreases during a local thermal fluctuation may be as high as 1500°F/sec. Although the strain resulting from these fluctuations is relatively small, the very high frequencies at which such a strain is cyclically applied may contribute to fuel element failure. Since bubble nucleation occurs preferentially at small surface crevices or pits, thermal cycling is focused on locations which are already sources of potential microcracks. The temperature will fluctuate at any fuel element surface experiencing nucleate boiling (either bulk or local). However, smaller fluctuations occur in a pressurized water system because of the higher pressure and greater forced convection cooling of the surface.

The relative importance of each of these mechanisms has yet to be fully assessed. However, controlled experiments are required to supplement engineering test data and to establish the relevance of these mechanisms to behavior of other cladding materials.

---

(1) F. D. Moore and R. B. Mesler, *A.I.Ch.E. J.*, 7: 4, 620 (1961).
(2) N. Madsen, Memo WWO 26-M31, Technische Hochschule, Eindhoven, 1964.
(3) T. S. Rogers and R. B. Mesler, *A.I.Ch.E. J.*, 10: 5 (September 1964).

R. J. Allio, Manager
Materials and Processes Development
Westinghouse Atomic Power Division

March 19, 1965

Section

I

Power Reactor Technology

Physics

Critical and Exponential Experiments

Several reports of results of critical and exponential experiments have been issued since the last review of the subject in *Power Reactor Technology* [7(3): 206-212 (Summer 1964)]. These include some papers from the Third Geneva Conference.

Reference 1 describes a series of critical experiments with a close-packed D_2O-moderated lattice in the Special Power Excursion Reactor Test II (SPERT-II). These experiments were directed toward providing information needed for design of the final operational core and for analysis of power-excursion tests conducted with that core to investigate the influence of prompt-neutron lifetime on reactor kinetics. In addition to the effects of initial system pressure and temperature, planned kinetic experiments with the close-packed core configuration will investigate the dynamic response of the reactor during forced coolant flow. Fuel assemblies, spaced on a uniform square pitch of 6.0 in., consisted of 3-in.-square thin-walled aluminum cans containing 18 highly enriched, removable, flat fuel plates separated by heavy-water channels 0.094 in. thick. The fuel plates were of a uranium-aluminum alloy meat (0.020 by 2.54 by 24 in.) clad with 0.020 in. of aluminum. Each plate contained a nominal loading of 7 g of ^{235}U, and therefore each assembly had a total of approximately 126 g of ^{235}U. The facility was designed to permit operation up to moderately elevated temperatures and pressures, e.g., 400°F and 375 psig, respectively. The reference discusses critical loadings, flux maps, adjoint flux maps, and the reactivity coefficients of pressure, temperature, and voids.

Bucklings were measured[2] by substitution techniques in the Process Development Pile for fuel assemblies composed of clusters of 19, 31, and 37 natural UO_2 rods with various rod spacings within the cluster. The UO_2 rods were 0.500-in.-diameter sintered pellets (10.4 g/cm^3) stacked in aluminum tubes having an outside diameter of 0.547 in. and a wall thickness of 0.020 in. The hexagonal rod clusters were placed inside aluminum-housing tubes of circular and hexagonal cross section and were of such dimensions as to limit the coolant-flow area to realistic values. The various coolants investigated were Dowtherm A, polyethylene, H_2O, air, and D_2O. The single-region reference-core loading consisted of 31-rod UO_2 clusters contained in D_2O-filled aluminum-housing tubes; both the reference and test lattices were spaced on a 9.33-in. triangular pitch. Measurements were made by the successive substitution technique wherein effective critical water heights are determined after the substitution of one, three, and finally seven test assemblies. One-group perturbation and two-group flux-matching methods were used in the interpretation of the experimental data.

Reference 3 presents a summary of experimental and theoretical results obtained in the Heavy Water Lattice Project of the Massachusetts Institute of Technology (MIT) during the period October 1962 to September 1963. Experimental methods were developed during previous studies on lattices of 1-in.-diameter natural-uranium rods in the main subcritical (exponential) assembly. These methods were employed in the evaluation of the material buckling, fast-fission effect, and resonance and thermal captures in fuel lattices of 0.25-in.-diameter slightly enriched-uranium-metal fuel rods. The uranium metal was enriched to 1.03% ^{235}U and was clad with aluminum 0.028 in. thick. Values of the material buckling were evaluated for unreflected lattices of the 1.25-in. triangular pitch in both the 3- and 4-ft-diameter tanks

and with a 2.50-in. triangular pitch in the 4-ft-diameter tank. Preliminary results on measurements of the ratio of fissions of ^{238}U to fissions of ^{235}U, and on the ratio of epithermal to thermal fission of ^{235}U, are reported for lattice pitches of 1.25, 1.75, and 2.5 in. Results are compared with earlier results obtained in the Miniature Lattice Facility at MIT and with results obtained at Brookhaven National Laboratory with 0.25-in. rods in lattices moderated by H_2O. Measurements of the ^{238}U cadmium ratio, the ratio of ^{238}U capture rate to the ^{235}U fission rate, and intracellular distributions of neutron-capture rates in ^{238}U and copper are described and compared, where possible, to measurements made in the Miniature Lattice Facility. Experimental determinations of intracellular thermal-neutron distributions and comparisons with analytical results are discussed. In particular, the difficulties arising from the cylindrical approximation to the unit cell, mainly with the lattices of 1.25-in. triangular pitch, the use of improved energy-exchange kernels, and modifications of the THERMOS code to include the effects of radial and axial leakage are described. The progress on miniature lattices, two-region or substituted lattices, and pulsed-neutron studies is also discussed.

Experimental data were obtained at both the Savannah River Laboratory (SRL) and the Hanford Laboratories to establish standards for the prevention of accidental criticality in handling, storing, and processing uranium metal enriched to 3 wt.% ^{235}U. In the Hanford experiments the approach-to-critical and exponential methods were used to provide material bucklings and critical masses for H_2O-moderated lattices with fuel-rod diameters of 0.175, 0.300, 0.600, and 0.925 in. The SRL measurements, discussed in Ref. 4, employed subcritical exponential techniques to determine the material buckling for H_2O-moderated lattices containing metal rods of 2- and 3-in. diameters at several lattice pitches. The material buckling for fuel elements of a given diameter and lattice pitch was evaluated from measured values of the neutron relaxation lengths along the axes of assemblies having at least two different effective diameters. The use of assemblies with different effective diameters permitted an evaluation of the radial extrapolation distance without the measurement of transverse flux shapes. Tabulations of the extrapolation distance, transverse buckling, neutron relaxation length, material buckling, and critical mass are given for the configurations investigated at SRL. A summary of both the SRL and Hanford data for the 3 wt.% ^{235}U metal rods is given in Ref. 4.

The ZPR-III facility has been used to study the properties of very large fast power breeder reactors by a two-zone-core technique wherein a small subcritical portion of a large dilute system is positioned in the center of the critical-facility matrix and surrounded by a buffer region and an annular driver region. Reference 5 describes the measurements in assembly 42 which were designed to assess the validity of this technique. The central core area of assembly 42 had an effective radius of 9.22 in., a length of 34 in., and a composition identical to that of a previously run dilute simulated uranium carbide reactor (assembly 34). The buffer region consisted of a 0.5-in.-thick depleted uranium filter with a length equal to that of the inner zone. Surrounding the buffer zone radially, and with an axial length equal to that of the two inner regions, was a driver zone of 3.18-in. nominal thickness. This driver zone had a ^{235}U volume fraction approximately twice that of the central core region. A depleted uranium blanket surrounded the entire core assembly in both the axial and radial directions. Reactivity measurements performed in this assembly included determinations of plate-orientation worth, homogeneity corrections, reactor-segment worths, central reactivity coefficients, and radial worth distributions of axial columns of core materials. Spectral-index determinations included central fission ratios, nuclear track emulsion measurements, fission-counter traverses, Rossi-alpha measurements, sodium activation, and natural- and enriched-uranium foil measurements. Comparisons between results obtained for the central core region and assembly 34 are given.

The second two-zone core built in the ZPR-III facility (assembly 43) is described in Ref. 6. In this case the central region with its low-density axial blanket was designed to simulate a projected fast power breeder reactor employing uranium monocarbide with a high proportion of ^{238}U to promote internal breeding. The basic structural and coolant materials were stainless steel and sodium, respectively. The composition of the driver region was so chosen that the complete assembly would be critical within the ZPR-III inventory of enriched ura-

nium. The composition of the buffer region was then chosen, by calculation, to modify the spectrum of the neutrons diffusing in from the driver to a spectrum similar to that in the central zone. The low-density axial blanket behind the central zone was identical in composition to the central zone except that the enriched uranium was replaced with stainless steel. The remaining part of the core was surrounded by a depleted uranium blanket. In both the central and driver zones, experimental determinations were made for sodium void coefficients and reactivity effects resulting from the substitution of enriched and depleted uranium, ^{233}U, ^{239}Pu, simulated fission products, and various structural and control materials. Spectral indices were measured, and reaction-rate traverses and activation experiments were performed. The reactivity change due to the Doppler effect was measured by heating a large depleted uranium oxide sample.

In support of the Advanced Sodium Graphite Reactor program, a series of critical and exponential experiments[7,8] has been performed to determine values of the material buckling and k_{eff} for graphite assemblies fueled with slightly enriched uranium carbide. These assemblies employed triangular lattice pitches of 9, 11, and 12 in. and, in most cases, included control-channel mockups. The uranium carbide fuel elements each contained 18 fuel rods arranged in two concentric rings about a centrally located, voided, stainless-steel tube. The inner fuel ring consisted of 6 rods evenly spaced on a 1.47-in.-diameter circle, and the outer ring consisted of 12 rods evenly spaced on a 2.84-in. circle. Each fuel rod contained a 72-in. stack of 0.500-in.-OD uranium carbide pellets inside a 0.010-in.-thick 0.550-in.-OD stainless-steel tube. The uranium carbide had a density of 13.23 g/cm^3, a carbon weight fraction of 4.9%, and a ^{235}U enrichment of 3.02%. The region outside the fuel rods and within the 0.025-in.-thick 4.00-in.-ID process tube was filled with sodium to a height of 72 in. The number of uranium carbide fuel elements (24) was much less than the number required for a bare or reflected critical assembly; consequently it was necessary to employ a driver region surrounding the test lattice to achieve a critical configuration. Fuel elements for the graphite-moderated driver region consisted of hollow cylinders (1.026 in. in inside diameter and 1.730 in. in outside diameter) of uranium metal enriched to 2 wt.% ^{235}U and stacked inside a 0.040-in.-thick aluminum tube. Fuel assemblies in the driver region were spaced on a 10.6-in. triangular pitch regardless of the lattice pitch employed in the test region. The critical experiments provided data on source multiplication measurements for the test lattices as well as on the number of driver assemblies required for each lattice to achieve criticality. The former data were used to determine the k_{eff} for each uranium carbide test lattice. Lattice configurations identical to those employed as test regions in the two-region critical assemblies were employed in the exponential measurements. In addition, data were also obtained for the same lattice compositions, but with reduced radial dimensions, to permit an evaluation of the effective radial buckling for a given lattice composition. Material-buckling values inferred from the two-region critical measurements are compared with those obtained from the exponential measurements and with those obtained by multigroup and few-group calculational schemes.

A short description of the critical and exponential facilities at the Institute of Nuclear Research, Swierk, Poland, as well as a brief description of the Institute's research programs, is given in Ref. 9. The critical assembly ANNA is a heterogeneous water-graphite-moderated pile with a graphite reflector. The central region of the graphite pile has 45 cylindrical holes positioned on a square pitch of 14 cm, into which graphite plugs or fuel channels can be inserted. Each fuel element is composed of three aluminum-canned coaxial tubes of 20% enriched UO_2. ANNA serves primarily as a mockup facility of the high-flux reactor. The MARYLA reactor is a zero-power (1 kw) flexible pool type facility designed for the study of various light-water systems. The individual fuel assemblies consist of 15 or 16 fuel pins, each of which is 8 mm in diameter by 50 cm long and contains 8 g of ^{235}U. HELENA is a subcritical assembly designed to investigate the parameters of natural-uranium–graphite lattices. The fuel is in the form of aluminum-canned uranium slugs, 30 cm long by 2.5 cm in diameter.

The NPY Project is a joint undertaking in reactor physics between the International Atomic Energy Agency and research laboratories in Norway, Poland, and Yugoslavia. Reference 10 presents a description of the NPY lattices studied, the experimental techniques

used in the measurements of neutron-flux distributions, and comparisons between the experimental flux distributions and theoretical predictions. The rod type fuel elements employed in the zero-power facility NORA (Kjeller, Norway) have a fuel radius of 5.64 mm and consist of nonsintered UO_2 powder which has a density of 9.28 g/cm^3 and which is enriched to 3 wt.% ^{235}U. The cladding is type 304 stainless steel with a thickness of 0.71 mm. The lattices reported were moderated by D_2O (99.4 mole %) and employed square pitches of 10, 4.908, and 3.658 cm. The lattices employed in the above-mentioned zero-power assembly ANNA (Swierk, Poland) consist of H_2O-cooled annular elements moderated by graphite and positioned at a square pitch of 14 cm. The fuel element is composed of an inner aluminum support tube, three concentric fuel annuli clad with aluminum, and an aluminum tube that separates the outer water annulus from the graphite. Each fuel annulus is 2.3 mm thick and is composed of 38.5 wt.% UO_2 (enriched to 20% ^{235}U) and 61.5 wt.% aluminum. The fuel element employed in the RB zero-power reactor (Vincha, Yugoslavia) consists of a single fuel annulus that is enriched to 2 wt.% ^{235}U, clad with aluminum, and moderated and cooled by D_2O. The D_2O coolant at both surfaces of the fuel annulus is separated from the inner and outer D_2O-moderated regions by thin-walled aluminum tubing. Square lattice pitches of 8 and 17.9 cm were investigated. Experimental data on thermal-flux distributions measured at the three facilities are compared with analytical results obtained by various calculational techniques, e.g., THERMOS, one-group Amouyal-Benoist, and one-velocity P_3.

Reference 11 is a description of the ROSPO critical facility (Comitato Nazionale per l'Energia Nucleare) that was built for the PRO power-reactor project to test organic-moderated cores. This facility was designed to carry out critical experiments in various cores differing in size, geometry, and control-rod type. During operation the moderator temperature can be changed over a range from about 40°C above the melting point to about 20°C below the boiling point, e.g., 190 to 350°C for Santowax OMP. Over this range the moderator temperature can be maintained constant to within ±0.5°C. The moderator level can be varied and controlled to ±1.5 mm. Data to be obtained by means of the ROSPO facility are as follows: critical-mass values vs. core configuration and fuel enrichment; temperature coefficients, control-rod worth, and reactivity effects associated with structural components. In addition to a detailed description of the facility, Ref. 11 gives data on the following for the first core: critical loadings, worth of control rods and peripheral fuel elements, and temperature-coefficient and buckling measurements. The first core is of the plate type and is moderated and cooled by Santowax OMP. The fuel assemblies are square boxes (71 by 71 mm) fabricated from 0.78-mm-thick stainless-steel sheet. The fuel plates are 96.4 cm long by 0.72 mm thick and 70 mm wide. The meat is an enriched (90% ^{235}U) UO_2 dispersion in an AISI type 304 stainless-steel matrix; the cladding is AISI type 304L stainless steel.

Reference 12 presents a summary of results obtained by pulsed-neutron techniques on graphite- and H_2O-moderated systems and critical experiments on H_2O-UO_2 systems. The pulsed experiments were made on two reflected, highly subcritical systems: (1) a graphite-moderated and -reflected system in the semihomogeneous critical assembly at the Japan Atomic Energy Research Institute (JAERI) and (2) the light-water-moderated UO_2 subcritical reflected system at the Mitsubishi Atomic Power Industries (MAPI) research laboratories. Reasonable agreement between calculated and measured values of the prompt-neutron decay constant of the fundamental mode was reported. The light-water lattice studies were made by the Ozenji Critical Facility (OCF, Central Research Laboratory, Hitachi, Ltd.) and the Tank-type Critical Assembly (TCA, JAERI). Fuel elements used in the experiments at the OCF facility were of the rod type, containing 10-mm-diameter UO_2 pellets sheathed in 0.8-mm-thick aluminum tubes. The UO_2 enrichments were 1.5 and 2.5% ^{235}U. Rod type fuel elements were also used in the TCA. These elements had an effective diameter of 12.5 mm and contained 2.6% enriched UO_2. The results discussed in Ref. 12 for the various experiments include critical masses, flux distributions, spectral parameters, lattice and water-gap peaking, temperature and void coefficients, and space-dependent reactivity effects of fuel.

Two additional papers (Refs. 13 and 14) presented at the Third Geneva Conference are reviews that cover the work on critical experiments in the United States since the Second Geneva Conference in 1958. The first paper[13]

covers in detail the field of fast reactor critical experiments, and the second[14] does the same for the work on D_2O-moderated systems. An extensive list of references is included in each paper.

Age and Diffusion-Length Determinations

Measured and calculated values of the flux age of fission neutrons to the indium resonance energy (1.44 ev) in graphite have been reported in Ref. 15. The measurements were made in 8-ft-high hexagonal graphite assemblies having effective diameters of 5 and 7 ft. The assemblies were centered on a cylindrical graphite thermal column which was 5 ft in diameter and which extended $3\frac{1}{2}$ ft above the core of the 2-kw AE-6 water-boiler reactor. The graphite in the experimental assemblies was of AGOT grade and was cast in the form of 4-ft-long hexagonal logs with a distance across flats of 4 in. The graphite density was 1.697 ± 0.004 g/cm^3 as determined from the total weight and as-built dimensions of the assemblies. Two fission sources were employed; the primary source was $3\frac{1}{2}$ in. in diameter, and the secondary source was 1 in. in diameter. Each was fabricated from 4-mil-thick uranium enriched to 93.2 wt.% ^{235}U and was covered on the top side with a 20-mil-thick cadmium disk that served as a sink for thermal neutrons transmitted through the source from the reactor thermal column. Detector foils were 1 cm square by 5 mils thick and were composed of 40% indium and 60% tin; the cadmium boxes were 40 mils thick.

The various corrections investigated[15] experimentally included source perturbations, detector-foil perturbations, nonisotropic foil activation, and epithermal leakage from the graphite assemblies.

Theoretical values[16] of the spatial moments of the slowing-down density distribution at the indium resonance energy were determined by the TYCHE code, which is an infinite-medium slowing-down Monte Carlo program written in FORTRAN. The effects of both inelastic scattering and anisotropic elastic scattering are included in the calculation. Detailed descriptions of the cross sections employed in the code are given in Ref. 16. Comparison with experimental results requires an evaluation of the flux age, τ^{ϕ}. The latter quantity is related to the slowing-down age, τ^{q}, by the method of Goldstein,* which utilizes the Grueling-Goertzel relation to couple flux and slowing-down density.

$$\tau^{\phi} = \frac{M_2^{\phi}}{6} = \frac{M_2^{q}}{6} + \beta$$

where $\beta = \dfrac{\gamma D}{\xi \Sigma_s + \gamma \Sigma_a}$

$$\gamma = 1 - \frac{\alpha (\ln \alpha)^2}{2\xi (1 - \alpha)}$$

$$\alpha = \left(\frac{A - 1}{A + 1}\right)^2$$

and the undefined symbols have the conventional definitions.

Table II-1 presents a comparison between the experimental and theoretical results described above and the previously reported values of the age in graphite. All results are normalized to a graphite density of 1.60 g/cm^3. The experimental values quoted for the present work (Ref. 15) were computed using a parabolic integration procedure over the experimental points as well as an extrapolation of the experimental points. Additional contributions to the uncertainty in the computed flux age including the uncertainties in graphite density, counting statistics, foil positioning, and extrapolated flux distribution. The comments in Table II-1, particularly those relating to the experimental references, give some indication of significant differences between the present and past work.

Measurements of the flux age of fission neutrons to the indium resonance energy in several zirconium-water mixtures are described in Ref. 17. The experimental techniques were similar to those employed in the measurement of the age of fission neutrons in H_2O [reviewed in *Power Reactor Technology*, 7(4): 331 (Fall 1963)]; i.e., the measurements utilized a plane fission source of finite dimension and effectively infinite-plane detectors to give a result equivalent to a measurement using axial detectors and an infinite-plane source. The fission source consisted of an enriched-uranium foil, $28\frac{3}{4}$ in. in diameter and 4 mils thick, masked down to

*H. Goldstein, J. G. Sullivan, Jr., R. R. Coveyou, W. E. Kinney, and R. R. Bate, Calculations of Neutron Age in H_2O and Other Materials, USAEC Report ORNL-2639, Oak Ridge National Laboratory, July 12, 1961.

Table II-1 AGE TO INDIUM RESONANCE ENERGY, FOR FISSION NEUTRONS IN GRAPHITE[15] (ρ = 1.60 g/cm^3)

	$\frac{1}{6}M_2$, cm^2	M_4, 10^6 cm^4	M_6, 10^{10} cm^6	Comments
Present work (Ref. 15)				
Experiment	307.8 ± 2.0	6.577	3.843	Foils, 1 by 1 cm; cadmium boxes, 40 mils thick
Theory	307.4 ± 1.0	6.59 ± 0.06	4.01 ± 0.09	Monte Carlo calculation
Experimental reference				
Fermi*	317.0			Large point source (293 g), thick (0.102 in.) cadmium boxes
Hill†	310.6 ± 3.0	6.89	4.4	Large (4 by 6.35 cm) foils, thick (0.135 in.) cadmium boxes
Davey‡	337.9			Source: planar distribution of natural-uranium rods
Hendrie§	312.6 ± 0.5	6.87	4.3	Uncertainty based in counting statistics only
Theoretical reference				
Joanou¶	305.0			Moments method
Goldstein**	304.0 ± 3.0			Monte Carlo calculation

*E. Fermi, J. Marshall, and L. Marshall, Slowing Down of Fission Neutrons in Graphite, CP-1084, Nov. 25, 1943.

†J. E. Hill, L. D. Roberts, and G. McCammon, Slowing Down of Fission Neutrons in Graphite, ORNL-187, Jan. 19, 1949.

‡W. G. Davey, J. C. Field, J. C. Gilbert, and A. L. Pope, An Experimental Study of the Slowing Down of Fissions Neutrons and the Diffusion of Thermal Neutrons in Graphite and in Heterogeneous Mixtures of Bismuth and Graphite, AERE-R/R-2501, March 1958.

§J. M. Hendrie, et al., Slowing Down and Diffusion Length of Neutrons in Graphite-Bismuth Systems, in *Progress in Nuclear Energy, Physics and Mathematics*, Series 1, Vol. 3, Pergamon Press, Inc., New York, 1959.

¶S. D. Joanou et al., Moments Calculations of the Fermi Age in Moderators and Moderator-Metal Mixtures, *Nucl. Sci. Eng.*, 13(2): 171-(1962).

**H. Goldstein, J. G. Sullivan, Jr., R. R. Coveyou, W. E. Kinney, and R. R. Bate, Calculations of Neutron Age in H_2O and Other Materials, ORNL-2639, July 12, 1961.

an effective diameter of 12 in. with cadmium. The homogeneous zirconium-water mixtures were simulated by 0.113-in.-thick zirconium plates arranged parallel to the fission source in a tank of water. The detector foils were $\frac{3}{4}$ in. in diameter by 0.005 in. thick and were composed of 40% indium and 60% tin; cadmium covers were 20 mils thick. In a given plane, parallel to the fission plate, the foils were spaced radially from the axis of symmetry of the experimental assembly. The relative infinite-plane activity $\phi(z)$ was obtained by numerical integration of the following equation:

$$\phi(z) = \int_0^\infty r\phi'(r,z)\,dr$$

where $\phi'(r,z)$ is the activity of a foil at a distance r from the axis of symmetry and in a plane at a distance z from the fission source. Detailed descriptions of the methods of data reduction and tabulations of data are given in the reference. For metal-to-water ratios, R, of 0.0, 0.348, 0.565, and 1.20, the measured ages are given by τ (cm^2) = 26.63 ± 19.23R.

Steady-state measurements of the effective thermal-neutron-absorption cross section and diffusion length in graphite, by means of a beryllium-antimony source, are reported in Ref. 18. The effective absorption cross section was evaluated by comparing the volume-integrated thermal-neutron distribution measured in a finite graphite assembly with that measured in an "infinite" water assembly containing the same beryllium-antimony source. Although this method does give a result relative to the absorption cross section of H_2O, it does not require any assumption as to the magnitude of the transport cross section of graphite. The diffusion lengths were also evaluated from the asymptotic flux distributions in both the graphite and water assemblies. The graphite assembly was an 8-ft-high stack of hexagonal AGOT-grade graphite logs forming a decahedron 12 ft across the flats. Since the finite dimensions of the graphite stack allowed thermal leakage in both directions, displaced source measurements were made to facilitate evaluations of leakage effects. A detailed discussion of the experimental procedures, data-reduction techniques, and correction factors, i.e., source absorption, foil depression, and leakage factors, are given in the reference. The average effective absorption cross section $\sigma_a(\hat{v})$, evaluated at the most probable velocity for a Maxwellian distribution at 20°C, was 4.42 ± 0.08 mb and is in good agreement with a value of $\sigma_a(\hat{v})$ = 4.38 mb deter-

mined by the use of the transport mean free path λ_{tr} (steady state) reported by Campbell.* The graphite cross section can be expressed as $\sigma_a = 0.01332\ \sigma_a(H)$, where $\sigma_a(H)$ is the absorption cross section of hydrogen. The average diffusion length, normalized to a graphite density of 1.60 g/cm^3 and measured in the direction parallel to the extrusion axis, was 54.77 ± 0.20 cm, and, in the direction perpendicular to the extrusion axis, it was 55.10 ± 0.15 cm. The former value is in good agreement with the values measured by Campbell in graphite assemblies on the thermal column of the AE-6 water boiler reactor, namely, 54.7 ± 0.3 cm, corrected to 55.02 ± 0.20 cm for infinite geometry by a diffusion cooling correction. The diffusion length for H_2O was 2.80 ± 0.02 cm.

Cross Sections

The fission cross section of ^{241}Pu becomes more important for neutron economy and long-term reactivity changes as fuel elements are developed to withstand increasing total exposures and more particularly if plutonium is recycled. Reference 19 reports measurements made with the Materials Testing Reactor fast chopper and presents the fission cross section of ^{241}Pu from 0.02 to 100 ev. A value of 962 ± 38 barns was measured at 0.0253 ev. Multilevel parameters to 10 ev are given. Reference 20 also reports ^{241}Pu fission cross sections, measured with the Rensselaer Polytechnic Institute linear accelerator. The range of measurement is from 2 to 100 ev, with sufficient resolution to permit multilevel analysis to be carried out for the neutron energies below 36 ev.

In Ref. 21, measurements of the integral cross section for the ^{9}Be$(n,2n)$ reaction in the upper end of the fission spectrum (above 2.7 Mev) are reported. The results are based on measurements of the total amount of helium produced during irradiation of BeO specimens in the Battelle Research Reactor. The value reported is 460 ± 60 mb.

The measurement was made as part of an investigation of the long-term effects of fast-neutron irradiation on polycrystalline beryllia. It is suspected that helium generated within the crystalline matrix may be the cause of the loss of mechanical strength that has been observed in BeO after high fast-neutron doses at temperatures in the range of 100 to 500°C. The $(n,2n)$ process is perhaps even more troublesome in beryllium metal because the resulting helium is responsible for the swelling of beryllium fuel jackets after substantial exposures at relatively high temperatures. The process is, of course, beneficial to the neutron economy of reactors that contain considerable beryllium in regions where the fast-neutron flux is high. The results reported in Ref. 21 are not inconsistent with the $(n,2n)$ cross sections assumed at the 1959 Conference on the Physics of Breeding (Ref. 22).

Measurements of cross sections for a number of threshold reactions, averaged over the ^{235}U fission spectrum, are reported in Ref. 23. The measurements were made by an activation technique. The target material was irradiated in a fission-flux converter, and a characteristic gamma emission from the product nucleus was counted. Most of the results of the measurements are summarized in Table II-2. The half-lives listed in the table were not measured in the experiments but were taken from other sources for use in reducing the data.

Table II-2 MEASURED AVERAGE CROSS SECTIONS FOR THRESHOLD REACTIONS IN A ^{235}U FISSION SPECTRUM[23]

Reaction	$T_{1/2}$	Gamma rays measured, Mev	Breeding ratio of gamma rays, %	Average cross section measured, mb
^{24}Mg$(n,p)^{24}$Na	15.05 hr	1.368	100	1.31 ± 0.06
^{27}Al$(n,p)^{27}$Mg	9.5 min	1.015	98	2.9 ± 0.5
^{27}Al$(n,\alpha)^{24}$Na	15.05 hr	1.368	100	0.60 ± 0.03
^{31}P$(n,p)^{31}$Si	2.56 hr			30.5 ± 1.2
^{32}S$(n,p)^{32}$P	14.3 days			60 ± 1.2
^{47}Ti$(n,p)^{47}$Sc	3.4 days	0.16	66	22.0 ± 1.5
^{48}Ti$(n,p)^{48}$Sc	44 hr	1.32	100	0.21 ± 0.016
^{54}Fe$(n,p)^{54}$Mn	314 days	0.835	100	66 ± 3.5
^{56}Fe$(n,p)^{56}$Mn	2.58 hr	0.845	99	0.90 ± 0.05
^{58}Ni$(n,p)^{58}$Co	71.3 days	0.81	100	105 ± 5
^{58}Ni$(n,p)^{58m}$Co	9.0 hr			30 ± 7
^{64}Zn$(n,p)^{64}$Cu	12.8 hr	0.51	38	27 ± 1.6
^{67}Zn$(n,p)^{67}$Cu	61 hr	0.184	45	0.9 ± 0.1
^{92}Mo$(n,p)^{92}$Nb	10.1 days	0.93	98	6.2 ± 0.4
^{95}Mo$(n,p)^{95}$Nb	35 days	0.765	99	0.13 ± 0.02

Neutron Thermalization

A general review of neutron thermalization, with attention to reactor applications, is given in Ref. 24. The paper also discusses various computer methods for representing scattering

*R. W. Campbell, Diffusion Length in SGR Graphite, USAEC Report NAA-SR-Memo-7415, Atomics International, May 29, 1962.

kernels and for determining the thermal-neutron characteristics in reactor lattices.

The "scattering-law" formulation for the handling of differential scattering data was discussed previously at some length in *Power Reactor Technology*, 6(1): 6-14 and 6(4): 46-53. New tabulations of scattering-law data (scattering cross section as a function of energy and momentum transfer) are given in Refs. 25 and 26 for H_2O and D_2O at temperatures of 22 and 150°C. The measurements were made at Chalk River with a neutron spectrometer with selected initial neutron energies ranging from 0.034 to 0.26 ev. A comparison with earlier measurements (Ref. 27) at 24°C shows good agreement; the later compilations (Refs. 25 and 26), however, cover a wider range of variables. Measurements made in the USSR on H_2O at 23 and 90°C, as well as measurements on monoisopropyl-diphenyl ($C_{15}H_{16}$) at 20°C are tabulated in Ref. 28.

References

1. J. A. McClure and R. L. Johnson, Critical Loading and Initial Static Experiments in the SPERT II Reactor with a Closed-Packed D_2O-Moderated Core, USAEC Report IDO-16996, Phillips Petroleum Company, June 1964.
2. F. D. Benton, Measurements of Bucklings and Void Effects in D_2O-Moderated, Organic- or H_2O-Cooled Lattices of UO_2 Rod Clusters, USAEC Report DP-873, E. I. du Pont de Nemours & Co., Inc., June 1964.
3. I. Kaplan, D. D. Lanning, and T. J. Thompson (Eds.), Heavy Water Lattice Project Annual Report, USAEC Report MITNE-46, Massachusetts Institute of Technology, Sept. 30, 1963.
4. W. B. Rogers, Jr., and F. E. Kinard, Material Buckling and Critical Masses of Uranium Rods Containing 3 Wt.% U-235 in H_2O, *Nucl. Sci. Eng.*, 20(3): 266 (November 1964).
5. P. I. Amundson, R. L. McVean, and J. K. Long, A Two-Zone Fast Critical Experiment (ZPR-III Assembly 42), USAEC Report ANL-6733, Argonne National Laboratory, January 1954.
6. J. M. Gasidlo, J. K. Long, and W. P. Keeney, Doppler Effect Measurements, Sodium Void Coefficients, and Critical Studies of a 5000-Liter Fast Power Breeder Reactor by the Two-Zone Method (ZPR-III Assembly 43), USAEC Report ANL-6838, Argonne National Laboratory, May 1964.
7. O. R. Hillig and D. W. Latham, Material Bucklings of Critical and Subcritical Uranium Carbide Fueled Graphite Assemblies, Part I, Experiment, USAEC Report NAA-SR-9771, Atomics International, Dec. 1, 1964.
8. E. R. Specht, Material Bucklings of Critical and Subcritical Uranium Carbide Fueled Graphite Assemblies, Part II, Theoretical Interpretation, USAEC Report NAA-SR-9772, Atomics International, Aug. 1, 1964.
9. L. Adamski, Z. Bajbor, W. Dabek, J. Koziel, and W. Suwalski, Critical and Exponential Assemblies at the Institute of Nuclear Research—Swierk, presented at the Third United Nations International Conference on the Peaceful Uses of Atomic Energy, Geneva, 1964, Paper A/Conf.28/P/807.
10. L. Adamski et al., Microscopic Neutron Flux Distributions in Unit Cells of Critical Assemblies of the NPY-Project, presented at the Third United Nations International Conference on the Peaceful Uses of Atomic Energy, Geneva, 1964, Paper A/Conf.28/P/499.
11. G. Bitelli, G. Gambardella, R. Martinelli, S. Nicosia, F. Orestano, A. Pulacci, E. Santandrea, P. Saya, and R. Zona, ROSPO—Organic Moderated Critical Experiments, presented at the Third United Nations International Conference on the Peaceful Uses of Atomic Energy, Geneva, 1964, Paper A/Conf.28/P/871.
12. K. Sumita et al., Subcriticality Measurements by Pulsed Method and Critical Experiments on Light Water System, presented at the Third United Nations International Conference on the Peaceful Uses of Atomic Energy, Geneva, 1964, Paper A/Conf.28/P/846.
13. F. W. Thalgott, J. K. Long, W. G. Davey, W. Y. Kato, S. G. Carpenter, H. A. Morewitz, and G. H. Best, Fast Critical Experiments and Their Analysis, presented at the Third United Nations International Conference on the Peaceful Uses of Atomic Energy, Geneva, 1964, Paper A/Conf.28/P/265.
14. J. L. Crandall, W. L. Brooks, I. Kaplan, F. L. Langford, Jr., and L. C. Schmid, Lattice Studies and Critical Experiments in D_2O Moderated Systems, presented at the Third United Nations International Conference on the Peaceful Uses of Atomic Energy, Geneva, 1964, Paper A/Conf.28/P/268.
15. R. W. Campbell, R. K. Paschall, and V. A. Swanson, The Age of Fission Neutrons to Indium Resonance Energy in Graphite, Part I, Experiment, USAEC Report NAA-SR-8683, Atomics International, June 15, 1964; also reported in *Nucl. Sci. Eng.*, 20(4): 445 (December 1964).
16. H. Alter, The Age of Fission Neutrons to Indium Resonance Energy in Graphite, Part II, Theory, USAEC Report NAA-SR-8684, Atomics International, Oct. 9, 1963.
17. R. K. Paschall, The Age of Fission Neutrons to Indium Resonance Energy in Zirconium-Water Mixtures, USAEC Report NAA-SR-9503, Atomics International, Sept. 15, 1964.
18. J. A. DeJuren, T. E. Stewart, and E. R. Specht, Measurements of Thermal Neutron Absorption Cross Section and Diffusion Length of Graphite Using an Sb-Be Source, USAEC Report NAA-SR-9803, Atomics International, Aug. 1, 1964.
19. T. Watanabe and O. D. Simpson, Low-Energy Neutron Fission Cross Section of ^{241}Pu, USAEC Report IDO-16995, Phillips Petroleum Company, June 1964.
20. T. Watanabe, M. S. Moore, O. D. Simpson, J. E. Russell, and R. W. Hockenbury, Experimental Measurements of the Fission Cross Section of ^{241}Pu, USAEC Report IDO-16976, Phillips Petroleum Company, Apr. 10, 1964.

21. F. F. Felber, Jr., D. R. Farmelo, and V. C. Van Sickle, The Integral $^{9}Be(n,2n)$ Cross Section, USAEC Report PWAC-433, Pratt & Whitney Aircraft Division, United Aircraft Corporation, May 19, 1964.
22. Wolf Haefele, The Fast Multiplication Effect Due to the $(n,2n)$ Reaction in Beryllium and Beryllium Oxide, in Proceedings of the Conference on the Physics of Breeding, October 19–21, 1959, USAEC Report ANL-6122, pp.163-176, Argonne National Laboratory.
23. J. W. Boldeman, Fission Spectrum Averaged Cross Sections of Threshold Reactions, *J. Nucl. Energy: Pt. A & B*, 18(8): 417-424 (August 1964).
24. J. R. Beyster, N. Corngold, H. C. Honeck, G. D. Joanou, and D. E. Parks, Neutron Thermalization and Reactor Applications, presented at the Third United Nations International Conference on the Peaceful Uses of Atomic Energy, Geneva, 1964, Paper A/Conf.28/P/258.
25. B. C. Haywood, A Compilation of the Scattering Law for Water at 22°C and 150°C, British Report AERE-R-4484, January 1964.
26. B. C. Haywood, A Compilation of the Scattering Law for Heavy Water at 22°C and 150°C, British Report AERE-R-4582, May 1964.
27. P. A. Egelstaff, Compilation of Early Scattering Law Data, British Report AERE-R-3931, January 1962.
28. V. I. Mostovoy, V. S. Dykarev, D. P. Eremeev, S. P. Ishmaev, I. P. Sadikov, Ju. S. Saltykov, V. A. Taraban'ko, and A. A. Chernyshov, Experimental Studies on Neutron Thermalization, presented at the Third United Nations International Conference on the Peaceful Uses of Atomic Energy, Geneva, 1964, Paper A/Conf.28/P/367.

Section

II

Power Reactor Technology

Fluid and Thermal Technology

Conduction

Reference 1 is a report on an analytical determination of the temperature distribution in long, cylindrical fuel elements cooled internally by several channels. This conduction problem has been treated in the past, and Ref. 2 is a recent article on the subject. The Ref. 2 article describes the derivation of the so-called ROB code for the determination of the steady-state temperature distribution for a heat-generating, circular cylinder cooled by a ring of holes. The ROB code provides for analytically calculating the temperature as a function of radius and azimuthal angle if the heat-generation rate in the cylinder is spatially independent. The particular geometry used in the ROB code is shown in Fig. II-1. The analytical derivation in Ref. 1 is similar to that

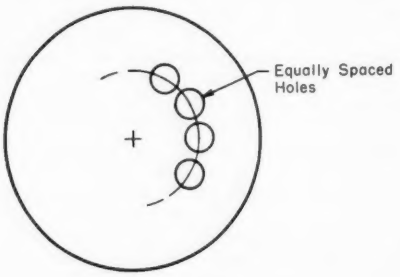

Fig. II-1 Cross section of cylinder illustrating geometry.[2]

in Ref. 2 except that a radially distributed heat-generation rate is provided for; Poisson's equation is solved by the method of "sources" and "sinks," with the assumption that the solid is isotropic. The reference presents the equations needed for calculating the temperature distribution for either an arbitrary radial distribution of the heat generation or a radial generation rate developed from neutron-diffusion theory.

Often in real cases the three-dimensional problem is important in elements of this kind; until the third dimension is incorporated into the analytical expressions, the designer must handle such problems as best he can. It may well be that the incorporation of a third dimension in the conduction equations would result in a prohibitively complex solution and that entirely numerical techniques will be required in calculation of the temperature distribution in the long, cylindrical fuel elements that are internally cooled.

References 3 and 4 present "large" conduction codes suitable for use on digital computing machines. Reference 3 presents a FORTRAN II code suitable for calculation of transient temperatures in a multiregion, axisymmetric, cylindrical configuration. The conduction code (ARGUS) allows up to 25 concentric regions, each region consisting of either a stationary or a turbulently flowing material having temperature-dependent properties. The stationary materials can have space- and time-dependent heat-generation rates, and temperatures are calculated at equally spaced nodal points. Material properties of the flowing materials are approximated by second-order polynomials. The thermal properties of the stationary materials must be constant except that, with appropriate heats of transformation, up to nine phase changes are allowed in these materials. Also allowed are 100 nodal points per radial row and up to 16 radial rows.

The IBM-650 code HEAT-1 presented in Ref. 4 is a one-dimensional time-dependent or steady-state heat-conduction code. The program obtains a numerical solution to the one-

dimensional heat-conduction equation in either slab or cylindrical coordinates by use of the finite-difference approximation to the partial differential equations. This program is somewhat smaller than the ARGUS code in that it can accommodate 10 regions and a maximum of 51 mesh points. The thermal conductivities and heat capacities are described by third-order polynomials, and a time-dependent and pointwise space-dependent heat source can be accommodated.

Apparently the thermal designer is accumulating a variety of machine codes that enable him to tackle many formidable conduction problems occurring in reactor design and analysis.

Reference 5 reports on the thermal conductivity of uranium dioxide fuel elements during irradiation. This reference deals with research at the Bettis Atomic Power Laboratory and is an extension of a program originally reported in USAEC Report WAPD-228. That report was reviewed in the March 1961 issue of *Power Reactor Technology*, 4(2): 39-43. Briefly the experiment was designed to measure the effective thermal conductivity of UO_2 and a zirconium oxide–uranium oxide mixture; the discussion here will be limited to those experiments employing only UO_2. Table II-1 gives the composition and density of the fuel materials used in the experiments, and Fig. II-2 illustrates the design of the capsule used for the in-pile measurements of the thermal conductivity. Table II-2 gives assembly and irradiation data on the several capsules. In Tables II-1 and II-2, the experiments designated "WAPD-22" are reported in WAPD-228, and the experiments designated "BETT" are reported in Ref. 5.

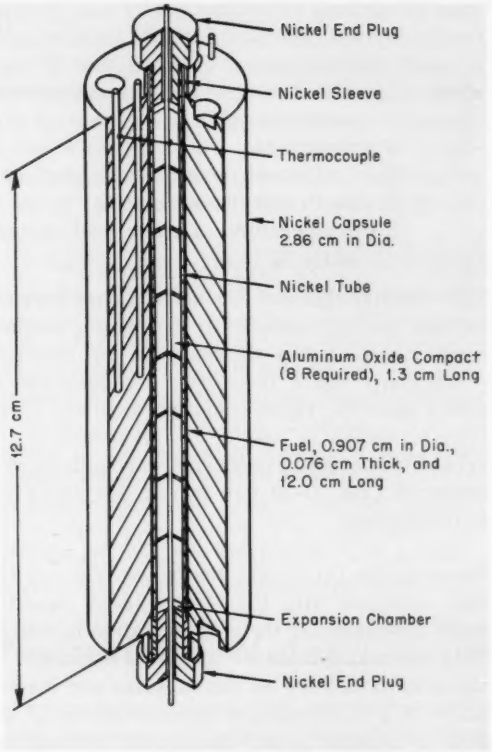

Fig. II-2 Capsule for in-pile measurement of the thermal conductivity of oxide fuels to high fission depletions[5] (BETT-69-4).

Table II-1 COMPOSITION AND DENSITY OF FUEL MATERIALS[5]

Experiment No.	Fuel	Wt.% ^{235}U in total U	^{235}U atoms/cm^3 ($\times 10^{-20}$)	Average fuel density	
				G/cm^3	% TD*
WAPD-22-11	UO_2 (natural)	0.7	1.65	10.4	95
BETT-69-1-C1	UO_2	21.0	50.0	10.6	97
BETT-69-4-C1	UO_2	21.4	51.0	10.6	97

*Percent of theoretical density.

The fuel cylinders were pressure bonded between the nickel capsule and a thin inner tube filled with BeO or Al_2O_3 (Fig. II-2). The capsule design was considerably different from the one employed for the WAPD-22 experiments, in which the fuel pellets were shrink fitted into type 304 stainless-steel capsules (Table II-2). The stainless-steel and nickel capsules had radial pairs of thermocouples for the determination of heat flux and a central thermocouple for the determination of the central temperature.

Figure II-3 illustrates BETT-69 capsule results for the effective thermal conductivity. The ordinate of Fig. II-3 shows the effective thermal conductivity, defined as follows:

$$K_{\text{eff}} = \frac{FP_f}{T_c - T_b} \quad (1)$$

where K_{eff} = effective thermal conductivity, watts/(cm)(°C)
F = constant
P_f = fuel power density, watts/cm^3
T_c = fuel center temperature, °C
T_b = temperature at inner wall of capsule, °C

The effective thermal conductivity thus depends on both the fuel conductivity and the gap-contact conductance, and a decrease in the effective conductivity could be caused by decrease in either quantity. These considerations are carefully explained in Ref. 5, and the observed decrease in the effective thermal conductivity with exposure (Fig. II-3) was indeed due primarily to irradiation.

Figure II-4 illustrates the contact conductances of the UO_2-metal interfaces. The earlier data obtained with the WAPD-22-11 capsules were reworked for their presentation in Ref. 5. This reworking involved improved estimates of the gamma heating of the capsules and the results of postirradiation determinations of the fuel-to-capsule gaps. Additional conclusions are quoted from Ref. 5 as follows:

1. The inpile thermal conductivities of UO_2 and $UO_2 + ZrO_2$ fuels at practical operating temperatures are essentially the same as their unirradiated conductivities up to fission depletions of about 10^{19} fissions/cc for operating temperatures near 500°C.

. . . . . .

3. For operating temperatures near 500°C, the thermal conductivities of UO_2, ZrO_2 + 34 w/o UO_2, and ZrO_2 + 46 w/o UO_2 decreased approximately 50, 25, and 35 percent, respectively, between 1×10^{19} and 25×10^{20} fissions/cc.

. . . . . .

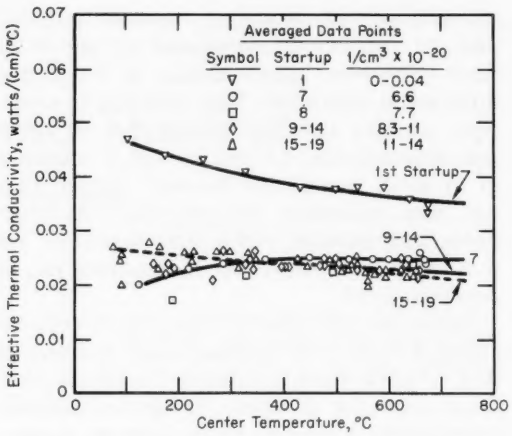

Fig. II-3 BETT-69-4 data for the effective thermal conductivity of UO_2 (Ref. 5).

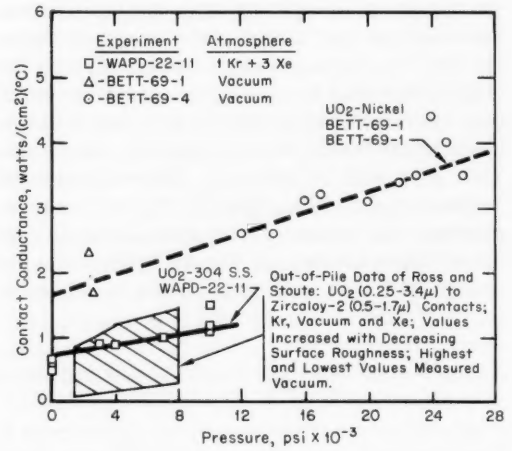

Fig. II-4 Contact conductances of UO_2-metal interfaces.[5]

Table II-2 ASSEMBLY AND IRRADIATION DATA[5]

Experiment No.	Capsule material	Gas-filling atmosphere	Fuel wall thickness, cm	Estimated total exposure, thermal neutrons/cm^2 ($\times 10^{-20}$)	Total burnup, fissions/cm^3 ($\times 10^{-20}$)	Remarks
WAPD-22-11	Type 304 S.S.	1 Kr + 3 Xe	0.365	4.0	0.35	Shrink-fitted fuel pellets
BETT-69-1-C1	Nickel	1 Kr + 3 Xe	0.365	2.0	5.4	Pressure bonded (thin internal cladding with powdered BeO in bore)
BETT-69-4-C1	Nickel	Vacuum	0.076	4.3	28	Pressure bonded (thin cladding supported by Al_2O_3 pellets shrink fitted after pressure bonding)

5. The initial inpile contact conductances of UO_2 + Zircaloy interfaces, derived from inpile data for UO_2 + nickel and UO_2 + type 304 stainless steel joints, are in good agreement with out-of-pile contact conductances of UO_2 + Zircaloy interfaces measured by Ross and Stoute [Canadian Report CRFD-1075]. Both the inpile data (for first start-ups) and the out-of-pile data indicate that, for interface pressures near 3000 psi, the contact conductance is approximately 1 watt/cm^2-°C for UO_2 + Zircaloy contacts between surfaces having surface roughnesses of less than 1 micron whether the interface is evacuated or filled with krypton and xenon. It is thought that the contact conductance decreases proportionally with the UO_2 conductivity, but additional data are needed to verify such decreases.

The thermal conductivity of uranium dioxide is also discussed in Ref. 6. This report presents an improved radial-heat-flow technique for the experimental determination of thermal conductivity, and a large section of the reference is a discussion of the technique and the results determined for Armco iron. However, the thermal conductivity of polycrystalline uranium dioxide was measured for the temperature range −57 to 1100°C. The uranium dioxide was prepared in the form of disks of nuclear-grade depleted UO_2 powder, cold pressed and sintered in hydrogen at 1850°C for 4 hr. The resulting pellets were 93.4% of the theoretical density (10.97 g/cm^3). The results indicated that the thermal resistivity, which is the reciprocal of the thermal conductivity, is linear between 200 and 1000°C with a slope of 0.0223 cm/watt. Between 1000 and 1100°C a slight deviation from the linear behavior was noted in the direction of increasing thermal conductivity, and the authors of Ref. 6 suggest that this may indicate a change in the composition of the material or a change in the basic heat-transport mechanism within the solid.

Gases

The following thermodynamic properties of helium are discussed in Ref. 7: pressure-volume-temperature and enthalpy relations, specific heat, viscosity, thermal conductivity, and Prandtl number. The compilation is an updating and expansion of previous work and includes recent information. In general, the property data are given for temperatures approaching 2000°F.

References 8 to 10 are British publications dealing with heat-transfer-coefficient calculations for gases at high temperatures. References 9 and 10 are not recent reports but have been included for completeness. The specialized case of heat transfer to superheated steam is presented in Ref. 11. This reference correlates data on the heat-transfer coefficient for superheated steam at 1000 psia flowing in a uniformly heated circular duct. The following expression is recommended for design purposes:

$$\mathrm{Nu}_b = 0.021\ \mathrm{Re}_b^{0.8}\ \mathrm{Pr}_b^{0.6} \left(\frac{T_b}{T_w}\right)^{0.575} \qquad (2)$$

In Eq. 2 the symbols have their usual meanings. The correlation suggests that, as the wall temperature (T_w) increases, the Nusselt number decreases. The functional relation, which is derived by the author of Ref. 11, results from a definition of the Reynolds number in terms of the bulk velocity, the density, and the viscosity at the film temperature. The correlation reproduces the data to within ±10%, although only 18 runs were used to establish the correlation.

Pressurized Water

Fragmentary information on pressurized-water research of general interest was reported by Oak Ridge National Laboratory (Ref. 12) and Hanford Atomic Products Operation (Ref. 13). A dimensionless correlation was developed[12] for predicting the critical-heat-flux value for natural-convection burnout of water in a heated vertical channel closed at the bottom and open at the top to a liquid supply. Data were taken with tubes which were operated at atmospheric pressure and which had inside diameters from 0.086 to 0.25 in. and lengths from 6 to 48 in. This physical situation, although not of interest in reactor operations, might be encountered during the shutdown and depressurization of a power reactor. The correlation given in Ref. 13 is for the pressure drop occurring during local boiling. The experiments were conducted with a 19-rod electrically heated bundle; flow rates varied from 500,000 to 5×10^6 lb/(hr)(sq ft) at a pressure of 1200 psia.

References 14 and 15 deal with heat transfer to a fluid flowing in an annulus; Ref. 14 is concerned with water, whereas Ref. 15 deals with an arbitrary coolant. Annular-flow heat transfer was treated in the March 1961 issue of *Power Reactor Technology*, 4(2): 13-15, and the conclusion in that review was that under cer-

tain conditions the effect of the diameter ratio on the heat-transfer coefficients of the inner- and outer-wall surfaces was uncertain. In particular, Fig. IV-1 in that issue illustrates that the discrepancies by and large were between results obtained in this country and results obtained by Russian experimenters. After deriving theoretical expressions for heat transfer in an annulus, the author of Ref. 14 presents experimental data on the heat-transfer coefficients of inner- and outer-wall surfaces using average wall temperatures and calculated bulk water temperatures. The important result seems to be that the ratio of film coefficients of the inner- and outer-wall surfaces is dependent on the heat-flux level and the ratio of the inner and outer values of the heat flux. Accordingly the situation is somewhat more complex than was suggested in the earlier review. The author of Ref. 14 states that the theoretical predictions of Maloney, appearing in what is cited as an unpublished work, adequately fit the experimental results.

The analysis given in Ref. 15 extends consideration to heat transfer in an annulus with a variable circumferential heat flux. The treatment is completely analytical, and no experimental data are given. The analysis takes into consideration the resistance to circumferential mixing, with the assumption that in turbulent flow the eddy diffusivity in the circumferential direction is the same as that in the radial direction. Although no experimental support is given, the condition of a circumferentially varying heat flux is the usual one encountered in reactors.

Reference 16 is a report on the transient behavior of a natural-circulation loop operating near the thermodynamic critical point. The particular fluid studied in the report was Freon-114, primarily because it had a low critical temperature (294.2°F) and because thermodynamic data for the material were available. The analytical portion of the study consisted of writing one-dimensional conservation equations for a control volume and stacking the control volumes to obtain the simulated loop. The system of equations thus obtained was solved with the aid of a high-speed digital computer. The computer model, however, failed to represent the system adequately, primarily because of the assumptions used when the model was set up. The flow-stability results, however, are probably of general interest, and the following quotation from Ref. 16 serves to define them:

> It has been determined experimentally that operation of a single-phase, heat-transfer loop in the thermodynamic critical region of the fluid of the design studied in this experiment will produce pressure and flow fluctuations under certain conditions. The condition determined experimentally for the occurrence of sustained flow and pressure fluctuations was that the system fluid be passing through the thermodynamic region in which a maximum in the density-enthalpy product as a function of temperature, enthalpy, or density occurs. In this region it was found that as little as $1\frac{1}{4}$ kw of heating was necessary to obtain sustained flow oscillations. The loop would operate stably in the thermodynamic regions on either side of this maximum in the density-enthalpy product. It was noted experimentally that the magnitude and frequency of the pressure and flow fluctuations depended on whether the maximum in the density-enthalpy curve was being traversed from the low- or the high-temperature side. Approach from the low-temperature side resulted in a dominant frequency of 10 to 20 cps, which was 100 times the frequency found when traversing the maximum from the high-temperature side.

Reference 17 deals with the critical, or burnout, heat-flux determination in subcooled, boiling water flowing under forced convection. The reference contains a number of arbitrary correlations, mostly derived by manipulation of the Jens-Lottes equation. The existence of a number of correlations probably is caused by the attempt to correlate data taken from systems operating in various subcooled-boiling flow regimes. This is recognized by the author,[17] and as many as four different regimes are postulated. These are the nucleate-boiling flow regime, the stratified-bubble flow regime, the nonstratified-bubble regime, and froth flow. The nucleate-boiling flow regime probably is the most straightforward of all. In this case, which occurs only at subcoolings greater than about 50 Btu/lb, the nucleate bubbles are rapidly quenched by the liquid flow stream. Occurrence of the regime requires also a system pressure of at least 500 psi, mass velocity in excess of 0.9×10^6 lb/(hr)(sq ft), and an equivalent diameter in excess of $\frac{1}{8}$ in. The stratified and nonstratified flow regimes are separated by a matter of degree rather than type, the stratified regime changing gradually to a nonstratified flow as the bubbles become dispersed in the bulk of the coolant. The stratified-bubble flow regime consists of unquenched bubbles which are concentrated close to the heat-transfer surface and which actively inhibit the frictional and heat-transfer effects of the turbulence caused by the nucleate boil-

ing. This "shield" minimizes the effect of the surface condition of the transfer surface, in contrast to the nucleate-boiling flow regime where a greater dependence of the critical heat flux with respect to the heat-transfer surface condition is encountered.[17]

Froth flow occurs at low subcoolings, with flow channels less than $\frac{1}{8}$ in. in diameter, or at pressures below 500 psi. The regime is characterized by relatively large amounts of unquenched bubbles, and the phase structures are somewhat similar to net vapor generation.

References 18 and 19 present design data pertinent to bundle type fuel assemblies. The particular geometry studied experimentally in Ref. 18 is illustrated in Fig. II-5; it consists of

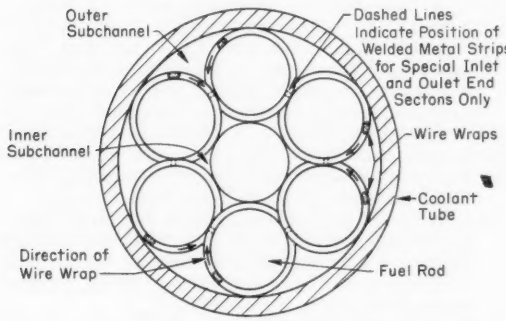

Fig. II-5 Cross section of a wire-wrapped seven-rod bundle in a coolant tube.[18]

a wire-wrapped seven-rod bundle placed within a flow tube. The spiral wire wrappings are typical of rod-bundle construction and serve not only to promote mixing between the coolant subchannels but also to help maintain proper spacing between adjacent rods and between the rods and the flow tube. The geometry shown in Fig. II-5 is particularly germane to pressure-tube type reactors. The experiment was conducted by injecting a salt solution into the inner coolant channels of a 70-in.-long seven-rod bundle fitted into the flow tube. Tap water was introduced into the outer coolant channels; and samples were taken of the outer-coolant-channel fluid at several places along the length of the bundle for analysis of salt concentration. The measurements then could be converted into a determination of the amount of coolant mixing that resulted for various wire-wrap configurations. The wire wraps produced considerable interchannel mixing, and the amount of mixing varied with changes in the wire-wrap pitch, although the amount was relatively insensitive to the relative spacing between the wires on adjacent rods.

Reference 18 presents equations to determine the interchannel coolant-mixing rate and gives two illustrative problems on the use of the equations in a practical reactor design. It is shown, for example, that the use of the wire wraps reduces the temperature inequality between the inner- and outer-coolant-channel streams (for the particular design study) by about a factor of 6. Reference 19 discusses the effect of wire wraps on the pressure drop for axial turbulent flow through rod bundles. The experiments reported in Ref. 19 were done with two basic types of assemblies: one was similar to the bundle shown in Fig. II-5, and the second incorporated a wire wrapped around the entire rod bundle as well as on the individual rods. A 19-rod bundle with wraps on 12 rods plus the overall bundle was also tested. Data were taken with unwrapped rods, and the increase in pressure drop caused by wrapping the rods in the fuel bundle is presented graphically in the reference. It was determined that the ratio of the pressure drop with wrapped rods to the pressure drop for the nonwrapped rods was proportional to the square of the number of wire wraps per unit length of rod. Changing the relative spacing between wires on adjacent rods caused some change in the pressure drop along the rod bundle. The entrance and exit losses across the rod bundle and end fittings are presented in tabular form, and the reference states that the data show only "fair agreement" with generally accepted contraction-expansion loss coefficients.

Organic Fluids

Reference 20 presents data on the heat-transfer properties of organic coolants containing high-boiling (HB) residues. The coolants studied were Santowax R (a mixture of terphenyl isomers), a mixture of Santowax R and HB residues produced by the pyrolytic decomposition of Santowax R, mixtures of Santowax R and HB residue from the Organic Moderated Reactor Experiment (OMRE), and OMRE coolant. Data were taken in the range of Reynolds numbers from 10^4 to 10^5 and were found to correlate within $\pm 8.5\%$ by an equation given in the reference. In addition, several experiments

were carried out under subcooled boiling conditions. The coolants used for the experiment were the OMRE coolant and a 55% pyrolytic HB-residue mixture. The authors conclude that subcooled boiling of organic coolants containing HB residues is a complex phenomenon since the multicomponent fluids have a very wide range of boiling points; it is concluded[20] that "the advantages to be gained by operating a reactor in this region may be marginal." This conclusion is based on the fact that as boiling commences the heat-transfer coefficient often decreases and does not return to its nonboiling value until the wall temperature is about 70°C higher than that needed to initiate boiling. Although this conclusion may be peculiar to the experimental conditions and apparatus used in Ref. 20, it is an important one and probably justifies additional study. The investigation wherein the decrease in heat-transfer coefficient with the onset of boiling was observed utilized the 50% pyrolytic HB-residue mixture; when the OMRE coolant was used as the working fluid, small increases in the heat-transfer coefficient were noted at the onset of boiling. In any case the operation of an organic system in the nucleate-boiling regime appears questionable.

References 21 and 22 deal with the determination of heat-transfer and void correlations during the forced-circulation boiling of organic coolants. Reference 21 is primarily a discussion of the test loop used to determine the data, although it contains a correlation of the forced-convection heat transfer of Santowax R and an isopropyldiphenyl mixture. The same coolants were used in the experiments reported in Ref. 22 to determine boiling-heat-transfer behavior, and Santowax R was used as a coolant in the void-fraction measurements. Coolant velocities from 5 to 14 ft/sec were utilized at system pressures from 15 to 35 psia. The boiling-heat-transfer data were compared with correlations of Levy, Rohsenow, and Forster-Greif. Graphical comparisons are given in Ref. 22, and, in general, the equation of Levy represented the data best. The void-fraction data for Santowax R were classified into three regions: region I covering subcooled boiling for coolant subcoolings greater than 8°F, region II covering the transition from subcooled equilibrium bulk boiling, and region III covering equilibrium bulk boiling at qualities greater than 0.005. A correlation is developed in Ref. 22 for the subcooled and transitional boiling, and the bulk-boiling void fraction was correlated with the Lockhart-Martinelli curve. The reference concludes with a discussion of the physical properties of isopropyldiphenyl and Santowax R.

References

1. D. E. Amos and F. R. Zaloudek, Temperature Distribution in Long Cylindrical Fuel Elements Cooled Internally by Several Channels, USAEC Report HW-77681, Hanford Atomic Products Operation, May 1963.
2. J. C. Rowley and J. B. Payne, Steady-State Temperature Solution for a Heat-Generating Circular Cylinder Cooled by a Ring of Holes, *J. Heat Transfer*, 86(4): 531-536 (November 1964).
3. D. F. Schoeberle, J. Heestand, and L. B. Miller, A Method of Calculating Transient Temperatures in a Multiregion, Axisymmetric, Cylindrical Configuration. The Argus Program, 1089/RE248, Written in Fortran II, USAEC Report ANL-6654, Argonne National Laboratory, November 1963.
4. R. J. Wagner, Heat 1—A One Dimensional Time Dependent or Steady State Heat Conduction Code for the IBM-650, USAEC Report IDO-16867, Phillips Petroleum Company, April 1963.
5. R. C. Daniel and I. Cohen, In-Pile Effective Thermal Conductivity of Oxide Fuel Elements to High Fission Depletions, USAEC Report WAPD-246, Westinghouse Electric Corp., Bettis Atomic Power Laboratory, April 1964.
6. T. G. Godfrey, W. Fulkerson, T. G. Kollie, J. P. Moore, and D. L. McElroy, Thermal Conductivity of Uranium Dioxide and Armco Iron by an Improved Radial Heat Flow Technique, USAEC Report ORNL-3556, Oak Ridge National Laboratory, June 1964.
7. D. R. Doman, High-Temperature Thermodynamic Properties of Helium, USAEC Report HW-78724, Hanford Atomic Products Operation, December 1963.
8. A. R. Pickering, Turbulent Heat Transfer to Fluids with Variable Physical Properties—A Review, British Report AEEW-R-290, February 1964.
9. N. Sheriff, P. Grumley, and J. France, Heat-Transfer Characteristics of Roughened Surfaces, British Report TRG-Report-447, Mar. 7, 1963.
10. A. C. Rapier, Forced Convection Heat Transfer in Passages with Varying Roughness and Heat Flux Around the Perimeter, British Report TRG-Report-519, Mar. 6, 1963.
11. W. A. Sutherland, Heat Transfer to Superheated Steam, USAEC Report GEAP-4528, General Electric Company, Atomic Power Equipment Department, May 1963.
12. Oak Ridge National Laboratory, July 7, 1964. (Unpublished)
13. M. M. Hendrickson and J. K. Green (Eds.), Research and Development Programs Executed for the Division of Reactor Development, Quarterly

Progress Report, July, August, September 1963, USAEC Report HW-79280, Hanford Atomic Products Operation, October 1963.

14. A. R. Pickering, Forced Convection Heat Transfer to Water in an Annulus, British Report AEEW-R-295, February 1964.
15. W. A. Sutherland and W. M. Kays, Heat Transfer in an Annulus with Variable Circumferential Heat Flux, USAEC Report GEAP-4571, General Electric Company, Atomic Power Equipment Department, May 1964.
16. Darrel G. Harden, Transient Behavior of a Natural-Circulation Loop Operating Near the Thermodynamic Critical Point, USAEC Report ANL-6710, Oklahoma State University, Argonne National Laboratory, and Associated Midwest Universities, May 1963.
17. R. J. Weatherhead, Nucleate Boiling Characteristics and the Critical Heat Flux Occurrence in Subcooled Axial-Flow Water Systems, USAEC Report ANL-6675, Argonne National Laboratory, March 1963.
18. E. D. Waters, Fluid Mixing Experiments with a Wire-Wrapped 7-Rod Bundle Fuel Assembly, USAEC Report HW-70178(Rev.), Hanford Atomic Products Operation, November 1963.
19. E. D. Waters, Effect of Wire Wraps on Pressure Drop for Axial Turbulent Flow Through Rod Bundles, USAEC Report HW-65173(Rev.), Hanford Atomic Products Operation, June 1963.
20. A. G. Debbage, M. Driver, and P. R. Waller, Heat Transfer Properties of Organic Coolants Containing High-Boiling Residues, Briti h Report AEEW-R-261, January 1963.
21. F. Bergonzoli (Ed.), Flow-Stability Test Loop, USAEC Report NAA-SR-8610, Atomics International, Mar. 1, 1964.
22. F. Bergonzoli and F. J. Halfen, Heat Transfer and Void Formation During Forced Circulation Boiling of Organic Coolants, USAEC Report NAA-SR-8906, Atomics International, June 15, 1964.

Section

III

Power Reactor Technology

Fuel Elements

Cermet Fuels for Fast Reactors

Development at the Oak Ridge National Laboratory (ORNL) of fuel-fabrication processes[1] for core B of the Enrico Fermi reactor has been concentrated[2] on 0.112-in.-thick flat cermet plates containing 35 wt.% UO_2 dispersed in, and clad with, type 347 stainless steel. Spheroidal oxide fuel particles with diameters of 105 to 149 μ (−100 +140 mesh) were used.[2] In the development program different tendencies for fragmentation and stringering were observed for different batches of the spheroidal UO_2 during roll-bonding operations. An attempt[3] was made to establish a specification that would permit the consistent purchase of spheroidal UO_2 with a high degree of reliability to minimize fragmentation and stringering during roll bonding. A number of control tests were devised in an attempt to characterize different batches of powder. The method of evaluation was to compare metallographically the stringering and fragmentation in rolled plates made with material from each batch of UO_2 with that of rolled plates fabricated with fused and ground material. Oxide batches with performances equal to or poorer than the standard were rated as unacceptable, and those with performances superior to the reference were classified in their relative order of quality. Results of the characterization tests reported in Ref. 3 are summarized as follows:

1. Microhardness. Good particles with low porosity and high bulk density cracked severely. No correlation with performance during roll bonding could be established.

2. Attrition. Correlations could not be established.

3. Crushing strength. Results of simple test procedures were capable of differentiating good from poor batches. Differentiation of a large amount of material in the intermediate category could not be made. However, it was felt that more exotic test procedures, requiring large expenditures of time and effort, might be developed to permit better differentiation of the intermediate batches.

4. Grain size. No correlations could be established.

5. Surface area. The Brunauer-Emmett-Teller (BET) method, using N_2 and krypton, was employed. No correlations could be found. It is interesting to note that differences as great as 40% were observed between BET measurements made at ORNL and fuel vendors, although repetitive measurements at ORNL exhibited reasonably high degrees of reproducibility.

6. Bulk density. Mercury-pycnometer measurements were capable of differentiating between the highest and lowest grades of UO_2 but were not capable of separating acceptable material from intermediate grades of UO_2.

7. Solid embedment. Density determinations on particles embedded in epoxy resin, when combined with empirical density corrections based on metallographic observations, provided the best correlations.

On the basis of the above evaluations, it was concluded that the mercury-pycnometer method would provide gross classification of obviously acceptable and unacceptable batches. A minimum density of 10.1 g/cm^3 was set as a lower limit for grade-A material, and material with a density below 9.8 g/cm^3 was classified as unacceptable. Material having intermediate densities was classified as grades B or C. The solid-embedment technique could then be used to classify batches between these limits.

Uranium dioxide powder that was classified[3] in various grades below the optimum, as a result of the preceding test procedures, was heated in hydrogen for 1 hr at 1750°C. Internal

porosity decreased, and the quality of all powder batches was increased as a result of this treatment.

A rolling temperature of 1200°C was previously established for the Fermi prototype fuel elements on the bases that the shape of the UO_2 particles was retained and that the condition of the plate surfaces was acceptable. A reevaluation of rolling temperatures from 900 to 1250°C was made[3] using the standard Fermi prototype rolling schedule, the best-rated UO_2 powder batches, and a loading of 33 wt.% UO_2.

Results are summarized as follows:

1. Surface finish. Rolling above 1050°C produced a mat finish, whereas lower rolling temperatures provided a satin-smooth finish that was free of pits.

2. Fragmentation and sintering. In all cases this was not excessive but increased with decreasing rolling temperature.

3. Density of cermet fuel. In all cases this was insensitive to the rolling temperature within the range evaluated.

4. Core-cladding bond. Bonding occurred at all temperatures. Grain coarsening became excessive at temperatures greater than 1150°C.

On the basis of the preceding results, it was concluded that the optimum rolling temperature was 1150°C. Other investigations[3] indicated that cold rolling severely fragmented the cermets made with either optimum- or poor-quality oxide and that fragmentation of the oxide was enhanced if too small an initial reduction was used in plate rolling. It was demonstrated[4] that the performance of fuel elements containing UO_2–stainless-steel cermets clad with stainless steel is, under thermal-cycling conditions somewhat comparable to those anticipated during large changes in reactor power levels, a function of the fabrication method employed. Investigations centered on stainless-steel-clad cermet fuel plates containing 40 to 50 vol.% UO_2. These studies included evaluation of hot compacted, as well as cold compacted and sintered, cermet cores and clad plates that were hot rolled at 1100°C to reductions in area from 60 to 90%. The cermet cores in these rolled plates were fabricated either from random-mixed or homogenized-mixed* cermet cores.

*Random-mixed cores are formed from mixtures of UO_2 and stainless-steel particles. Homogenized-mixed cores are formed from mixtures of stainless-steel powder and UO_2 spheres which have been precoated with stainless-steel powder.

The thermal-cycling tests performed[4] on these materials employed a hot-leg temperature of 800°C with the cold leg either at 250°C or at room temperature. Holding times and transfer times were varied in the different tests; however, the most significant results were obtained from tests of up to 1000 cycles at a heating rate of 60 to 70°C/sec and a cooling rate of 250°C/sec.

Examination of the as-rolled plates indicated excessive stringering in the random-mixed cores and a relatively uniform dispersion of the UO_2 in the homogenized-mixed cores. Stringering in the random-mixed cores increased with increasing reductions. In the homogenized-mixed cores, there was no evidence of large agglomerates, stringering, or cracking of the UO_2. Performance of the homogenized-mixed samples during cycling was superior to that for the random-mixed cores. Sigma-phase formation was observed in the type 316L stainless-steel core. The amount of sigma increased with increasing number of cycles and was probably associated with the amount of time at 800°C in each cycle. On the basis of the observed distribution of carbides and sigma phase after cycling, it was concluded that these would not be deleterious to performance.

Although additional details are not given in Ref. 4, it is stated that new fabrication methods had been developed to produce plates of improved quality which would provide better thermal-cycling stability.

It was concluded[4] that stainless-steel-clad cermets containing 40 to 50 vol.% UO_2–stainless steel, prepared by the homogenized-mixed-core process, could withstand 1000 thermal cycles up to 800°C at heating and cooling rates up to 70 and 250°C/sec. The following conditions must be met[4] to provide good resistance to thermal cycling:

1. Elimination of continuous interparticle networks in the core

2. Use of spheroidal UO_2 that is well dispersed in the core

3. Use of spheroids with minimum internal stress and high resistance to fragmentation

4. Good initial bonding between cermet core and picture-frame cladding

The use of Dynapak and a combination of Dynapak plus swaging is under development[5] at Los Alamos for the fabrication of refractory-metal-clad 45 vol.% UO_2–tungsten cermet fuels. The program is aimed at determining the fea-

sibility of coextruding refractory-metal-clad cermet fuel elements. Work has been concentrated on a cermet made from 2-μ tungsten powder and 20-μ UO_2 powder which was hydrostatically pressed into $1\frac{1}{4}$-in.-diameter cylinders at either 50,000 or 70,000 psi. These compacts were induction sintered at 2200°C for 2 hr. Slow heating (4 hr) and cooling ($2\frac{1}{2}$ hr) cycles were required to minimize thermal-stress cracking. After the pellets were sintered, they were machined to dimensions of 1 in. in diameter by 1 in. long; their density was 85% of theoretical. Coextrusion billets were prepared by loading the machined pellets with a light press fit into cans of either molybdenum, 70 wt.% molybdenum–tungsten, or 25 wt.% molybdenum–tungsten and then electron-beam welding the lids. These billets were extruded in air, with glass wool as a lubricant, after they were preheated in H_2 to about 2000°C. Typical conditions included a fire pressure of 750 to 900 psi, velocity at contact from 460 to 540 in./sec, and extrusion ratios of 4 to 9. Typical yields ranged from 75 to 100% for finished lengths and diameters from $4\frac{3}{4}$ to $7\frac{1}{4}$ in. and 0.47 to 0.75 in. Although the cermet bond was uneven as a result of the penetration of UO_2 particles into the cladding, core-to-cladding bonding was generally good for all rods, and the bond quality increased with increasing extrusion ratio.

One rod clad with 25% molybdenum–tungsten and coextruded to a reduction in area of 89% was further reduced 75% in area by swaging at 1800°C (first third of reduction) and then at 1500°C. The surface appearance and bond quality were good. It was indicated that further reductions were possible.

It was suggested[5] that improvements in both fabrication and performance could be achieved with a 25 wt.% molybdenum–tungsten alloy for the cermet as well as for the cladding. Advantages claimed for this alloy are compatibility with H_2 and UO_2, availability, low relative cost, good high-temperature strength, and a melting point in excess of 3100°C. Furthermore, this alloy is less dense and is simpler to fabricate than tungsten. The success to date with Dynapak extrusions, as well as the potential advantages that can be gained through the use of the 25 wt.% molybdenum–tungsten alloy, have led to suggested programs at Los Alamos involving the extrusion of other shapes, the use of higher UO_2 loadings, and thinner cladding.

Fabrication of Various Fuel Assemblies

As part of the Fuel Cycle Program of the U. S. Atomic Energy Commission (AEC), the Atomic Power Equipment Department (APED) of the General Electric Company initiated a program aimed at extending the performance capabilities of UO_2 fuel elements in boiling-water reactors. Under this program 12 special assemblies have been fabricated and inserted in the Vallecitos Boiling Water Reactor (VBWR) for irradiation testing. Detailed descriptions of the fabrication of 3 of these special assemblies are given in Refs. 6, 7, and 10. The APED work under the Fuel Cycle Program has been reviewed previously in *Power Reactor Technology*, 7(1): 27-50, and 7(4): 354-355. The reports reviewed here present fabrication details not available when the earlier reviews were prepared; some repetition has been allowed for convenience of reading.

The AEC Fuel Cycle Special Assembly 8L, containing 16 fuel rods in a 4 by 4 array, was aimed[6] at demonstrating the performance of very thin (0.005 in.) type 304 stainless-steel cladding. The selection of the 0.005-in.-thick cladding for the program was based upon the realization that this represented the thinnest available stainless-steel tubing capable of performing a cladding function. Of the 16 fuel rods in the 8L assembly, 12 contained UO_2 with thin cladding. The corner rods had heavier cladding (0.015 in.) to reduce the probability of damage to the fuel assembly during handling. The 12 test rods, about 46 in. long, contained 4.58% enriched-UO_2 pellets which were 0.370 in. in diameter and which were clad with $\frac{1}{4}$-hard stainless-steel tubing. A 7-in.-long fission-gas plenum was designed to accommodate 100% gas release at twice the target burnup. In an effort to minimize wrinkling of the cladding, the cladding was swaged over the pellets, providing a nominal rod diameter of 0.380 in. Target heat flux and burnup were 500,000 Btu/(hr)(sq ft) and 10,000 Mwd/ton, respectively. At this heat flux a differential diametral expansion between the fuel and the cladding of 0.0035 in. was calculated, which would result in plastic straining of the cladding. Cladding-stress calculations, materials specifications, element design, cladding fabrication and evaluation, fuel-pellet fabrication, fuel-rod fabrication, and results of preirradiation tests

are discussed and described in detail in Ref. 6. Irradiation testing of this special element was begun in November 1961 and was terminated in December 1963 as a result of the final shutdown of the VBWR.

The AEC Fuel Cycle Special Assembly 9L contained UO_2-molybdenum cermet fuel.[7] Molybdenum additions were made in an attempt to increase the thermal conductivity of UO_2. Vacuum hot-pressing techniques were used to produce the two types of cermet pellets utilized in this assembly: (1) pellets containing 20 vol.% molybdenum fibers had densities of 94 to 95% of theoretical and (2) pellets fabricated from molybdenum-coated UO_2, containing approximately 16 vol.% molybdenum, had densities of 84 to 96% of theoretical. Radial orientation of the molybdenum fibers in the pellets was achieved by means of unidirectional compaction. Hot pressing of the molybdenum-coated UO_2 particles provided a continuous molybdenum network. The forms of UO_2-molybdenum cermets selected for the program were based on the intent to cover the largest possible range of difference in the mode of metal-phase distribution. Three fuel rods fabricated with each of the two types of uranium-molybdenum cermets were combined with two rods of conventional UO_2 pellet design to form the eight-rod Special Assembly 9L. All fuel cladding was type 304 stainless steel with an outside diameter of 0.515 in., a wall thickness of 0.020 in., and a pellet-to-cladding diametral clearance of 0.003 to 0.004 in. The objective of this test was to compare the performances of the cermet fuels and UO_2 after operation at a surface heat flux of 500,000 Btu/(hr)(sq ft) and a burnup approaching 15,000 Mwd/ton. Irradiation testing was begun in the VBWR in September 1962 and was terminated at the final shutdown of the VBWR in December 1963. The impetus for this series of irradiation tests was based on out-of-pile thermal-conductivity data[8,9] obtained for UO_2-Mo and UO_2-ThO_2-Nb (10 to 30 vol.% metal) which indicated potential improvements of 300%. Calculations of axial and radial temperature profiles anticipated for the cermet rods and the bulk UO_2 rods indicated substantial differences. Relative performance could then be judged by an analysis of microstructure data. Details of these calculations, as well as fuel-element-design characteristics, materials specifications, fabrication procedures, and results of preirradiation evaluations, are given in Ref. 7.

The AEC Fuel Cycle Special Assembly 11L contained[10] sintered UO_2 extrusions prepared independently under two different projects. One project was sponsored by the United States–Euratom Joint Research and Development Program at Compagnie Industrielle des Combustibles Atomiques Frittés (CICAF). The other project was a joint effort of the Allis-Chalmers Mfg. Co. and The Electric Autolite Co. (AC-EA) as part of the AEC Fuel Cycle Program. Fuel densities achieved were 97.6 and 96.2% of the theoretical density for the CICAF and AC-EA sintered extrusions. A 16-rod (4 by 4) assembly was fabricated for testing in the VBWR at a surface heat flux of 400,000 Btu/(hr)(sq ft). It contained 12 rods fabricated with sintered extrusions (6 from each program) and 4 pellet rods for comparison. The cladding was $\frac{1}{8}$-hard type 304 weld-drawn stainless steel with an outside diameter of 0.540 in. and a wall thickness of 0.022 in. Extrusion processes, descriptions of extrusions, fabrication and assembly procedures for fuel rods, irradiation design criteria, materials specifications, and results of preirradiation examinations are reported in considerable detail in Ref. 10. Results of some of the VBWR irradiations are summarized in two 1964 Geneva Conference papers (Refs. 11 and 12).

Hanford has published detailed specifications for swage compaction[13] and vibratory compaction (VIPAC)[14] of mixed oxide (UO_2-PuO_2) fuel in Zircaloy cladding for the Mark I-M, 19-rod clusters being irradiated in the Plutonium Recycle Test Reactor (PRTR). Fuel for the swaging process and the VIPAC process is a mixture of UO_2 and PuO_2 formed by a high-energy-rate pneumatic-impaction (NUPAC) method that yields fuel particles with a density greater than 97% of the theoretical density.

Ten full-sized sodium-bonded uranium carbide fuel assemblies of hypostoichiometric composition were fabricated[15] by Atomics International for testing in the Hallam Nuclear Power Facility. The objectives of the program, in addition to the irradiation testing of sodium-bonded fuel elements in the Hallam reactor, included the development of fabrication methods for carbide, the evaluation of storage conditions for cast carbide, and the development of sodium-bonding techniques and nondestructive test methods.

Each clad fuel rod[15] was about 182 in. long and 0.952 in. in diameter and contained a

uranium carbide fuel column 0.872 in. in diameter and 156 in. long. The radial sodium annulus between the fuel and the type 304 stainless-steel cladding was 0.030 in.; helium gas at 1 atm occupied the region above the sodium level. Each fuel assembly contained eight fuel rods. Uranium carbide enrichment in eight assemblies was 3.7%, and in the remaining assemblies, 4.9%. One of the eight assemblies with the 3.7% enrichment contained thermocouples located within the fuel and on the cladding surface.

The fabrication and inspection methods used for these sodium-bonded fuel elements are described in detail in Ref. 15. A number of significant observations are summarized below:

1. Uranium dioxide feed was converted to UC melt stock by the carbothermic reaction.

2. Better control of carbon content was attained for melt stock containing less than 500 ppm oxygen. The melt stock of lower oxygen content gave less splatter of the melt on the graphite electrode and thus less erratic carbon pickup.

3. Compensation of carbon pickup from the electrode was made by means of uranium-metal additions.

4. Metallographic determinations of carbon content near stoichiometric (4.6 to 4.8 wt.% carbon), based on comparison with controls, were more accurate than the analytical methods employed.

5. Dry storage was demonstrated to be effective, provided that prescribed fuel-preparation and fuel-storage conditions are followed.

6. Dry cutting methods were developed.

7. Proper fuel cleanliness was a necessary prerequisite for good sodium bonding.

Zircaloy-2-clad tubular fuel elements containing thorium–2.5 wt.% uranium (93.2% enriched)–1 wt.% zirconium fuel alloy were fabricated[16] for irradiation testing in the P-7 high-temperature high-pressure water loop of the Engineering Test Reactor (ETR). Fabrication development, including arc-melting techniques, coextrusion procedures, metallurgical evaluation, and fuel-element-assembly procedures, is described. It was shown that the zirconium addition to the base fuel composition improved the surface quality of arc-cast ingot, improved uranium homogeneity, lowered the fuel-alloy hardness, and was beneficial in consumable-electrode fabrication. Fully bonded tubular fuel, 1.750 in. in outside diameter by 1.050 in. in inside diameter with 0.025-in.-thick Zircaloy cladding on both the outside and inside diameters, was produced by coextrusion at 760°C at a reduction ratio of 17 to 1. Fuel elements 8 in. in length were closed by brazing Zircaloy-2 end caps with 5 wt.% beryllium–Zircaloy-2 alloy, followed by electron-beam welding of the braze line. Three fuel elements were charged in the P-7 loop in April 1963 and were operating at a maximum specific power of 230 kw/ft, a peak heat flux of 1.12×10^6 Btu/(hr)(sq ft), and a maximum calculated fuel temperature of 620°C. Interim measurement of fuel density will be made throughout the irradiation in which the target has a burnup of 3 at.%, or approximately 26,000 Mwd/ton.

Information on the potential for plutonium-enriched fuel in pressurized-water reactors will be obtained[17] as a result of the Saxton Plutonium Project. Nine fuel assemblies containing PuO_2-UO_2 are to be irradiated at the center of the Saxton core, and 12 stainless-steel-clad assemblies containing UO_2 are to be irradiated at the core periphery. Two of the plutonium fuel assemblies will contain PuO_2-UO_2 fuel that has been vibratorily compacted into Zircaloy-4 tubes; the remaining plutonium fuel assemblies will contain PuO_2-UO_2 pellets in a Zircaloy-4 cladding. Zircaloy was selected over stainless steel as the cladding material for the plutonium-containing elements because it provides higher initial reactivity and longer lifetime for a given plutonium enrichment. Equal heat ratings are contemplated for both types of plutonium-containing fuel elements. Descriptions of the fuel and fuel rods are summarized in Tables III-1 and III-2. Nuclear Materials & Equipment Corp. will supply the pelletized plutonium-containing fuel elements, and the VIPAC fuel elements will be fabricated[17] by Hanford from feed material prepared by the Dynapak process.

Table III-1 FUEL-ROD DETAILS FOR THE SAXTON PLUTONIUM PROJECT[17]

	Plutonium	Uranium
Cladding material	Zircaloy	304 S.S.
Cladding thickness, in.	0.023	0.015
Cladding outside diameter, in.	0.391	0.391
Diametral gap, in.	0.005 for pelletized 0.0 for VIPAC	0.004

Table III-2 FUEL DETAILS FOR THE SAXTON PLUTONIUM PROJECT[17]

Material	6 wt.% PuO_2–94 wt.% UO_2	6 wt.% PuO_2–94 wt.% UO_2	UO_2
Type	Pelletized	VIPAC	Pelletized
Diameter, in.	0.340	0.345	0.357
Density, % of theoretical	94	88	93
Enrichment	6 wt.% Pu	6 wt.% Pu	5.7 wt.% ^{235}U

Isotopic content of Pu, %	
^{239}Pu	90.46
^{240}Pu	8.60
^{241}Pu	0.90
^{242}Pu	0.04

Insertion of the plutonium-containing fuel assemblies in the Saxton reactor is scheduled for July, and plans are that these fuel assemblies will be irradiated for two years. Post-irradiation examination and analysis are scheduled for the period January 1968 to February 1969. A maximum fuel-rod heat rating of 16 kw/ft has been established[18] for the Zircaloy-4-clad PuO_2-UO_2 fuel rods. The following comments on hydrogen pickup and oxide thickness on the cladding are quoted from Ref. 17:

> The hydrogen pickup by the Zircaloy clad and the thickness of the ZrO_2 coating formed in-pile were calculated for linear rod powers of 16 kw/ft and assuming 40% down time for the reactor. The results showed that the hydrogen level at the end of life, 130 ppm, will be considerably below the level at which hydride problems occur. The ZrO_2 coating thickness and the temperature drop across the coating were found to be negligible.

Also from Ref. 17 a survey of performance of VIPAC fuel in other test programs is summarized as follows:

> 1. Based on technology already developed at the national laboratories, no defects in vibrationally compacted fuel rods are anticipated.
>
> 2. The results of the national laboratory experiments show that no significant fuel washout and no waterlogging results from defects in rods containing loose powder fuel.
>
> 3. The economic incentives for developing vibratory compacted PuO_2-UO_2 fuels and the present state-of-the-art provide strong motivation for carrying out engineering demonstration tests in the Saxton reactor.

References

1. J. E. Cunningham et al., Specifications and Fabrication Procedures for APPR-1 Core II Stationary Fuel Elements, USAEC Report ORNL-2649, Oak Ridge National Laboratory, Feb. 11, 1959.
2. J. H. Cherubini et al., Fabrication Development of UO_2–Stainless Steel Composite Fuel Plates for Core B of the Enrico Fermi Fast Breeder Reactor, USAEC Report ORNL-3077, Oak Ridge National Laboratory, Apr. 18, 1961.
3. A. J. Taylor et al., Characterization of Spheroidal UO_2 Particles and Studies of Fabrication Variables for Core B Fuel Plates of the Enrico Fermi Fast Breeder Reactor, USAEC Report ORNL-3645, Oak Ridge National Laboratory, August 1964.
4. J. M. Davies and C. Steer, Thermal Cycling of UO_2–Stainless Steel Cermets, British Report AERE-M-1253, January 1964.
5. J. M. Dickinson and T. J. Ready, Feasibility Study of the Co-Extrusion of Refractory Metal Clad Reactor Fuel Elements, USAEC Report LAMS-3065, Los Alamos Scientific Laboratory, Apr. 12, 1964.
6. J. P. Hoffman, Design and Fabrication of Pellet Fuel Rods Clad with Thin-Wall Stainless Steel, USAEC Report GEAP-4407, General Electric Company, Atomic Power Equipment Department, February 1964.
7. S. Y. Ogawa, AEC Fuel Cycle Program — Design and Fabrication of Special Assembly 9-L, Irradiation Performance Test of UO_2-Cermet Fuel, USAEC Report GEAP-4435, General Electric Company, Atomic Power Equipment Department, March 1964.
8. S. J. Paprocki et al., Preparation and Properties of UO_2 Cermet Fuels, USAEC Report BMI-1487, Battelle Memorial Institute, Dec. 19, 1960.
9. Y. Baskin et al., Some Physical Properties of Thoria Reinforced by Metal Fibers, *J. Am. Ceram. Soc.*, 43: 489-492 (September 1960).
10. F. H. Megerth, Design and Fabrication of Fuel Rods Containing Sintered UO_2 Extrusions, Assembly 11L, USAEC Report GEAP-4556, General Electric Company, Atomic Power Equipment Department, February 1964.
11. S. Naymark and C. N. Spalaris, Oxide Fuel Fabrication and Performance, presented at the Third United Nations International Conference on the Peaceful Uses of Atomic Energy, Geneva, 1964, Paper A/Conf.28/P/160.
12. W. P. Chernock, R. M. Mayfield, and J. R. Weir, Jr., Cladding Materials for Nuclear Fuels, presented at the Third United Nations International Conference on the Peaceful Uses of Atomic Energy, Geneva, 1964, Paper A/Conf.28/P/255.
13. Hanford Atomic Products Operation, Specifications for Swage-Compacted, Mixed Oxide (UO_2-PuO_2), Fuel Elements for the PRTR (Mark I-M), USAEC Report HW-79290, Oct. 1, 1963.
14. Hanford Atomic Products Operation, Specifications for Vibrationally Compacted, Mixed Oxide

(UO_2-PuO_2), Fuel Elements for the PRTR (Mark I-L), USAEC Report HW-79291, Oct, 1, 1963.
15. W. Draganchuk, UC Fuel Element Design and Fabrication, USAEC Report NAA-SR-9988, Atomics International, Aug. 1, 1964.
16. R. S. Kemper et al., Fabrication of Zircaloy-2 Clad Thorium–Uranium Alloy Fuel Elements, USAEC Report HW-79843, Hanford Atomic Products Operation, March 1964.
17. N. R. Nelson, Saxton Plutonium Program, Quarterly Progress Report for the Period Ending September 30, 1964, USAEC Report WCAP-3385-1, Westinghouse Atomic Power Division, October 1964.

Section

IV

Power Reactor Technology

Components

EBR-II Control-Drive Mechanisms

The Experimental Breeder Reactor II (EBR-II) is controlled by 12 hexagonal-shaped control subassemblies, moved vertically by 12 rack-and-pinion type electromechanical drive mechanisms. These are capable of scramming the control assemblies with an acceleration of 1.5 *g*, with a pneumatic cylinder providing the assist to attain this acceleration. The design stroke for the mechanism is 14 in. The control assembly was described in the EBR-II hazards summary report (Ref. 1) that was issued in May 1957. Some of the novel features of the mechanism (shown in Fig. IV-1) are as follows:

1. The mechanism has internal and external bellows seals that are fabricated from 0.010-in.-thick stainless-steel sheet to maintain vessel integrity.

2. A sensing-device shaft is used to indicate whether the control assembly is engaged to the mechanism. This sensing shaft is housed within the 26-ft-long main shaft.

3. A pneumatic cylinder at the top of the main shaft is used to accelerate the control assembly during a scram. Normal pressure in the cylinder is 30 psig.

4. An oil-filled dashpot decelerates the control assembly during the final $4\frac{1}{8}$ in. of scram.

5. All the control-assembly drive mechanisms are mounted on a single platform. This platform can be raised 3 in. to check the control-assembly grippers to ensure that they are disengaged and are clear of the adapters of other subassemblies in the core. The platform is lowered $\frac{7}{8}$ in. from its normal operating position to engage the control assemblies.

6. A labyrinth seal is used to limit the flow past the shaft bearing in the vessel cover.

Extensive testing was performed on 2 prototype drive mechanisms and on 1 of the 14

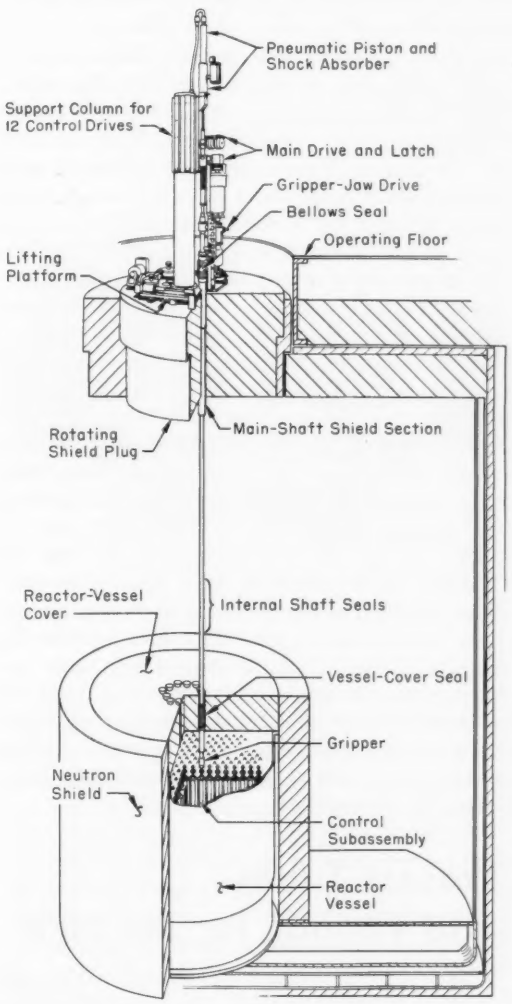

Fig. IV-1 Simplified drawing of components of the EBR-II control-rod drive.[2]

production mechanisms that were fabricated.[2] Table IV-1 summarizes the testing details.

Table IV-1 CONTROL-MECHANISM TESTING[2]

Rod	Environment	Temperature, °F	No. of full-stroke cycles	No. of gripper operations	No. of scrams
P-1	Air	Room	300		
	Sodium	300 to 900	13,200		24
P-2	Air	Room	31,440		
	Sodium	300 to 900	1,680	15	35
F-1	Air	Room	900	20	120
	Air	800	700	6	5
	Sodium	750	1,100	18	80

All these tests were performed with no significant problems. Furthermore, all the production rods were tested in place, and only minor adjustments were required. However, during a recent scram of the EBR-II, 2 of the 12 rods became stuck (rods 7 and 9).[3] Rod 9 was broken loose by applying a 200-lb force. The rod was then exercised by using a lifting force of 350 to 550 lb and slight mallet taps to assist its downward travel. After some exercise it resumed normal operation. Rod 7 required the fabrication of special tools to break it loose. It was determined that the main shaft for the rod was sticking in a $29\frac{1}{8}$-in.-long Stellite sleeve in the reactor-vessel cover. This sleeve is the lower guide bearing for the control-assembly shaft (Fig. IV-2) and also serves as a seal between the sodium inside the reactor vessel and the bulk storage outside the vessel. So that the leakage can be reduced, each main shaft contains 23 labyrinth grooves, as shown in the figure. The nominal radial clearance between the outside diameter of the main-shaft lands and the inside diameter of the sleeve is 0.015 in. It is reported in Ref. 3 that a special tool, which applied axial and rotational forces to the stuck shaft, performed successfully the task of loosening the seized shaft.

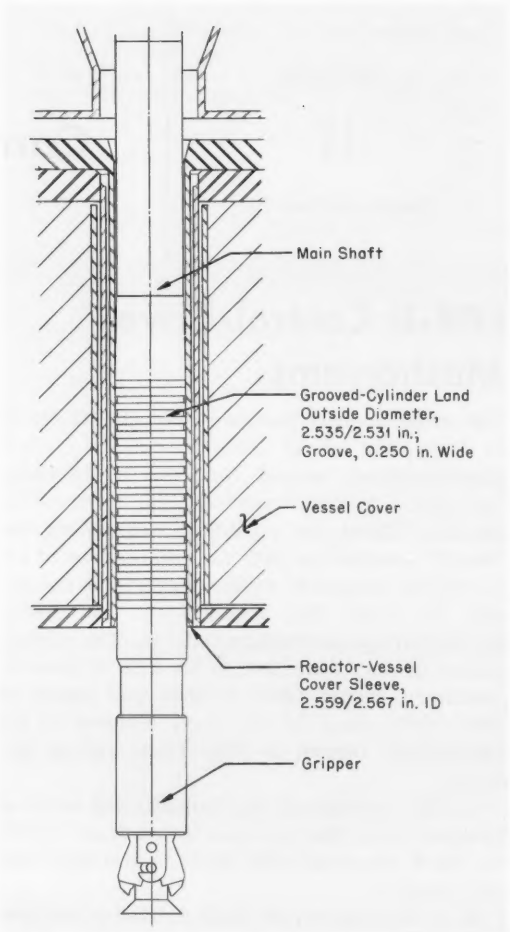

Fig IV-2 Main-shaft seal through the EBR-II reactor-vessel cover.[2]

Process Tubes and Fittings for the NPR

The New Production Reactor (NPR; also called the N Reactor) is a graphite-moderated pressure-tube reactor designed to operate at a coolant pressure of 1600 psi and a temperature of 300°C. The reactor requires 1064 Zircaloy-2 pressure tubes that are 57 ft long, 3.25 in. in diameter, and 0.25 in. in wall thickness, as well as a considerable number of fittings, connectors, and transition joints. Reference 4 is a descriptive summary of a development pilot order and a competitive-bid program for procurement of the pressure tubes. The procedures used for this program were required because of the lack of manufacturing technology and industrial experience with this relatively high-cost material and because of the stringent quality and dimensional requirements specified.

The initial phase of the program consisted of developmental contracts to three vendors on a best-efforts basis. The second, or pilot order, phase was awarded to the three vendors on a negotiated basis. The final phase was accomplished on the basis of a competitive-bid,

product-guaranteed, fixed-price contract. This procurement effort developed an industrial capability for producing heavy-walled Zircaloy tubing to reactor-application specifications[4] and covered the full range of processes from ingot to finished product. The effort included the development of (1) specifications that indicate the level of quality to which such tubing can be produced and (2) commensurate inspection and quality-control requirements.

Technical problems in the selection, manufacture, installation, and testing of primary-loop fittings are discussed in Ref. 5. The fittings included the rolled-joint connections between Zircaloy and carbon steel, a mechanical "make-and-break" coupling, a venturi assembly, manifold piping, and valve-body material. The leak-tight roller joint, shown in Fig. IV-3, was

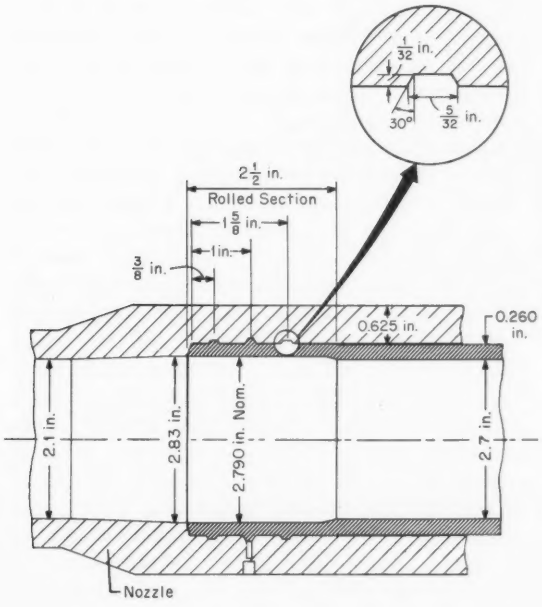

Fig. IV-3 NPR inlet rolled joint.[5]

designed for 1800 psi at 600°F and to withstand thermal shock from sudden coolant-temperature changes. This joint was selected over eight other mechanical type joints on the basis of superior strength and low-leakage qualities. In this type of connection, the Zircaloy tube is rolled into the grooved carbon-steel nozzle by means of an expander mandrel that provides for a 12% wall-thickness reduction. The rolling process forces Zircaloy into the grooves and provides a joint that is judged to be structurally sound and reliably leakproof.

The quick-connection make-and-break mechanical coupling was required to minimize the maintenance time at the faces of the reactor. Of 15 various candidate assemblies evaluated, the Grayloc type coupling was chosen for this application because of its ruggedness and resistance to leakage under different stress conditions and its clean internal-surface configuration. It features a two-stud split-clamp arrangement that causes axial loading of a tapered metal-seal member within the tapered bores of the coupling flanges. Spherical convex nuts and temporary shims are used during assembly of the coupling to minimize cocking and to maintain parallelism. Figure IV-4 shows the connector-coupling components.

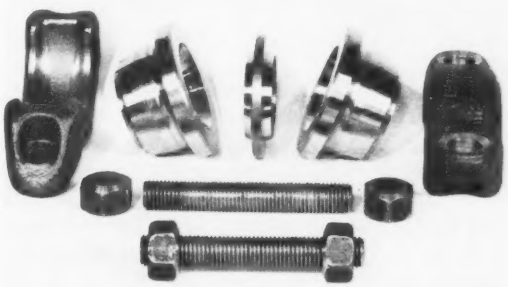

Fig IV-4 NPR connector-coupling components.[5]

The venturi throat assembly is used to monitor continuously the coolant flow in each of the connector pipes. The original design of this component specified a type 316 stainless-steel throat section to be mounted in a carbon-steel body by means of an interference fit. However, subsequent heat-treating operations caused loosening of the throat. The design was modified by substituting Inconel for stainless steel on the throat section, thus minimizing the differential thermal expansion. Extending the tap connection into the throat component corrected the loosening of the throat component.

The manifold piping on the NPR consists of over 100,000 ft of carbon-steel tubing of $2^5/_8$-in. outside diameter by 0.260-in. wall thickness. The piping connects the individual process tubes

to the 18-in. inlet and outlet headers. The connectors did not meet impact-strength requirements after bending. This deficiency was attributed to limitations of the heat-treatment equipment used in the manufacture.[5] It was subsequently corrected by additional heat-treatment, and thereafter the tubing met specified impact-strength requirements. The valve bodies of both forged and cast types failed to meet the impact-strength requirements specified. In some cases an additional grain-refinement treatment at 1550°F completely refined the structure, and notch toughness was raised above minimum values. In other cases detailed analysis of the metallurgical deficiency showed the need for a much more extensive modified heat-treatment procedure, in addition to some pre-heat-treatment machining operations, to bring the product above specified impact- and tensile-strength values.

References

1. L. J. Koch, W. B. Loewenstein, H. O. Monson, D. Okrent, M. Levenson, W. R. Simmons, J. R. Humphreys, J. Haugsnes, and V. C. Jankus, Hazard Summary Report, Experimental Breeder Reactor-II, USAEC Report ANL-5719, Argonne National Laboratory, May 1957.
2. E. Hutter and G. Giorgis, Design and Performance Characteristics of EBR-II Control Rod Drive Mechanisms, USAEC Report ANL-6921, Argonne National Laboratory, August 1964.
3. Argonne Staff, Reactor Development Program Progress Report, October 1964, USAEC Report ANL-6965, Argonne National Laboratory, Nov. 15, 1964.
4. T. C. Aungst and D. H. Curtiss, Procurement of Zircaloy-2 Process Tubes for N-Reactor, USAEC Report HW-80566, Hanford Atomic Products Operation, March 1964.
5. Staff of the N-Reactor Project, Technical Problems in Fittings for N-Reactor Primary Loop, USAEC Report HW-79616, Hanford Atomic Products Operation, November 1963.

Section

V

Power Reactor Technology

Specific Reactor Types

Large Pressurized-Water Reactors

The trend toward interconnected power systems in the electric-utility industry has greatly increased the opportunities for reducing unit power-generating costs through the use of very large plants. This trend has also focused attention on the question of the maximum capacity available from a single reactor in a nuclear plant. References 1 and 2 present the results of a study by the Westinghouse Atomic Power Division for the U. S. Atomic Energy Commission (AEC) to evaluate the technical feasibility and economic potential of a 1000-Mw(e) all-nuclear power plant incorporating a single pressurized-water reactor. The work was performed during the period May 1962 to March 1963. The results of the study command particular attention since the work was clearly based on the extensive Large Closed Cycle Water Reactor Research and Development (LRD) Program that Westinghouse has been conducting since 1960 in association with the San Onofre Nuclear Generating Station of the Southern California Edison Company. It is stated that the design philosophy adopted for the study represents a modest extension of the technology to be employed in the 375-Mw(e) Southern California Edison* and the 465-Mw(e) Round 3A† plants. The conclusion from the study is that the 1000-Mw(e) reactor is technically feasible and economically practical and that 1970 is a reasonable date for the commercial operation of the plant. A $10.5 million research and development program is outlined. The principal development problems lie in the area of core physics and core development and result from the increased core size.

Except for size the plant is similar to the present generation of pressurized-water reactors under contract, such as those for the San Onofre and Malibu stations. The plant has the following capabilities:

Reactor, Mw(t)	3220
Gross electrical generation, kw	1,058,000
Net electrical generation, kw	1,002,400
Cycle heat rate, Btu/kw-hr	10,377
Full-load net station heat rate, Btu/kw-hr	10,363
Net plant efficiency, %	31.1

Of the principal reactor-plant components, only the reactor vessel represents a measurable extension of present-day fabrication techniques. Although the 615-ton vessel can be shop fabricated and erected at the hypothetical site selected for the study,‡ transportation might be a limitation for less favorable sites. The pressure-vessel-design condition was 2500 psi at 650°F, and the vessel was to be designed, manufactured, inspected, and stamped in accordance with Sec. VIII of the *ASME Boiler and Pressure Vessel Code*. Since this study was completed, Sec. III, Rules for Construction of Nuclear Vessels, was approved and issued by the American Society of Mechanical Engineers. A discussion of the principal difference between the two code sections is presented in Ref. 3. The new Sec. III permits better utilization of the reactor-vessel material, resulting in a lighter weight vessel. For example, a reduction of more than 2 in. in thickness of the 202-in.-ID cylindrical section of the 1000-Mw(e) vessel can be achieved. Reference 3 concludes that the new code permits design of nuclear vessels for water-reactor plants up to 1500 Mw(e).

*The Malibu Plant of the City of Los Angeles Department of Water and Power.

†The Connecticut Yankee Atomic Power Company.

‡The "Middletown" site employed in the AEC evaluation studies of utility reactors since 1959.

In the design study presented in Ref. 1, seven primary coolant loops are employed. Each loop contains a vertical U-tube steam generator having 32,726 sq ft of heat-transfer surface and a canned-motor single-speed centrifugal pump with a design flow capacity of 61,000 gal/min against a 280-ft head. The pump volute contains an integral center-guided check valve positioned between the suction nozzle and the impeller. No main coolant block valves are used. In present-day plants the use of the block valves seems to be a customer choice; Connecticut Yankee uses them, but Malibu does not. The main coolant piping is 27-in.-ID rolled and welded carbon steel clad internally with stainless steel. The 3240-cu ft pressurizer vessel is connected to the hot leg of one reactor loop. The steam-generator design data are tabulated in Table V-1.

Table V-1 DESIGN DATA[1] FOR STEAM GENERATOR

Type	Vertical U tube with integral steam drum
Heat-transfer load, Btu/hr	15.729×10^8
Steam flow, lb/hr	2.014×10^6
Design pressure, tube side, psia	2500
Operating pressure, tube side, psia	2050
Tube material	Inconel
Coolant flow in each side, lb/hr	22.86×10^6
Coolant inlet temperature, °F	598
Coolant outlet temperature, °F	546
Shell-side full-load pressure at outlet, psia	700
Full-load steam temperature at outlet, °F	503
Maximum moisture at outlet (full load), %	¼
Shell-side design pressure, psia	1000
Feedwater temperature at full load, °F	442
Logarithmic mean temperature difference, °F	65.5
Heat-transfer surface area, sq ft	32,726
Dry weight, lb	503,800
Flooded weight, lb	738,800

The reactor-plant containment is provided by a reinforced-concrete vertical right-circular cylindrical structure with a flat base and hemispherical dome. The dome has an inside radius of 81 ft, and the total inside height is 211 ft. The structure is lined with a steel membrane ¼ in. thick to make the container vaportight and gastight. The containment is similar in design to the one built at Parr Shoals for the Carolinas-Virginia Nuclear Power Associates, Inc.

The turbine-generator represents a significant extension of current practice. The turbine is of 4-cylinder single-shaft design, operates at 1800 rpm, and turns a single 1,300,000-kva hydrogen-intercooled generator. The throttle pressure condition is 650-psia saturated steam as in current practice. Exhaust from the single double-flow high-pressure cylinder passes through six moisture separators and is reheated with steam at the throttle condition before being expanded in the three double-flow low-pressure cylinders. The entire high-pressure-turbine casing and the last five stages of each low-pressure-turbine casing are lined with stainless steel to minimize moisture corrosion. The low-pressure-turbine rotors are too large to ship completely assembled. The last two stages of each low-pressure turbine are bladed in the field. Similarly, because of size and weight, final assembly of the generator rotor and stator is performed in the field.

The estimated power-generation cost for the plant based on a net generation of 1,002,400 kw is 5.77 mills/kw-hr, made up as follows:

Capital	3.42
Land, working capital, and nuclear insurance	0.27
Fuel	1.83
Operation and maintenance	0.25
	5.77

The estimated total capital cost of the plant is $165,084,000, including land and land rights, interest during construction, and contingency; the resulting unit cost is $165 per kilowatt. The 1.83 mills/kw-hr fuel cost is based on an equilibrium core utilizing zirconium-clad fuel. The first-core fuel-cycle cost for the reference elastically collapsed stainless-steel-clad core is 2.13 mills/kw-hr. The first-core fuel-cycle cost for the alternative freestanding stainless-steel-clad core is 2.23 mills/kw-hr. Fuel cost estimates were based on government ownership of uranium.

The principal improvements and advances over current pressurized-water-reactor technology are in the area of the core and the associated reactor arrangement. Two designs were carried through in the study. The reference design utilized short Zircaloy followers for the control-rod blades and elastically collapsed thin-walled stainless-steel cladding on the fuel. The less-advanced alternate design

employed full-length control-rod followers and freestanding stainless-steel cladding. Slightly enriched UO_2 is used as fuel in both designs. The alternate design resulted in an increase of reactor-vessel length of 8 ft. The consequent increase of reactor-coolant-system holdup was 9%, and the increase in plant-container volume was 11%. The estimated capital-cost saving incurred by choice of the reference design is approximately $3 million. Figure V-1 shows the reactor-vessel assembly for both the reference and the alternate designs.

The reference-design core is roughly cylindrical in shape with an active height of 11 ft and an equivalent diameter of 12.8 ft. The individual fuel elements consist of UO_2 pellets, 0.354 in. in diameter by 0.708 in. high, enclosed in stainless-steel tubes of 0.010-in. wall thickness. The cladding operates under an elastically collapsed condition, as described in Ref. 1:

In order to reduce the amount of steel in the reactor core and improve neutron economy, elastically collapsed 304 stainless steel was selected for the clad material. The normal fuel rod has an inside diameter of 0.358 inches with a wall thickness of 0.010 inches ±0.0005. The collapsed clad is designed to be elastically buckled between 1000 – 1500 psia pressure. At zero power conditions the maximum stress in the clad will be localized at the inner surface of the vertices of the buckled clad and will approach the yield strength of the material. However, it is expected that the clad will be pushed back toward a circular shape by the fuel pellets as the reactor is brought from zero power to full power and that the maximum clad stress will be below the yield strength during normal operations.

The fuel assemblies of the reference core consist of a basic 16-by-16 square array of fuel rods with 20 rods omitted from the periphery of the assembly to provide space for control rods. A cross section of the fuel assembly and control rod is shown in Fig. V-2. The outermost row along the periphery of each

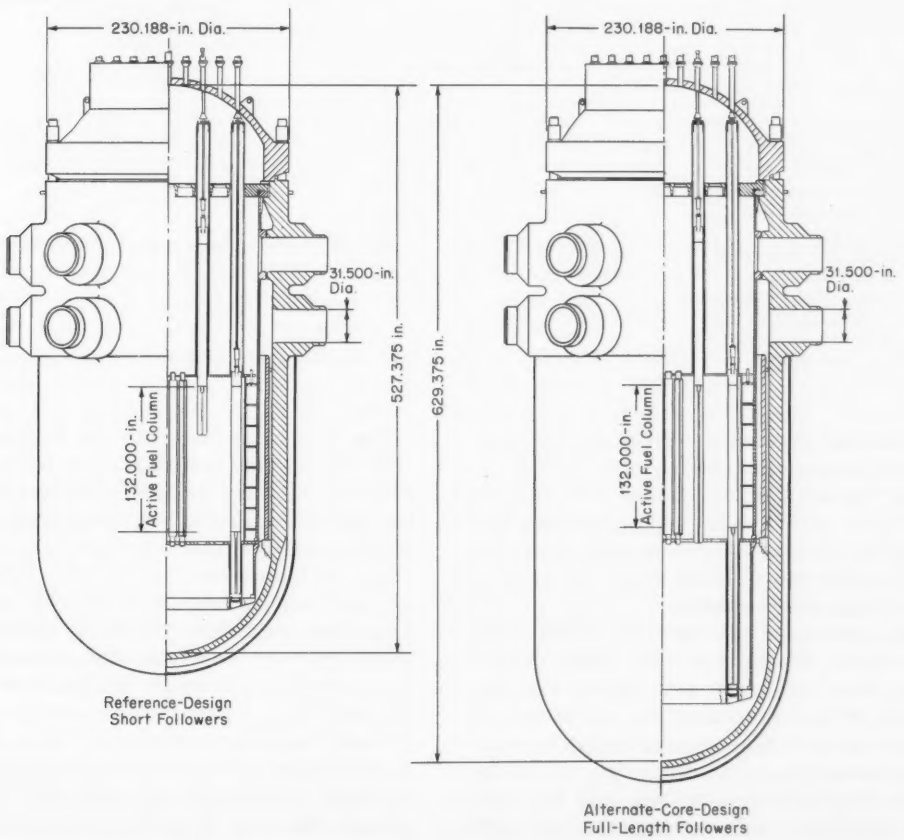

Fig. V-1 Reactor-vessel assembly for both the reference and alternate designs.[1]

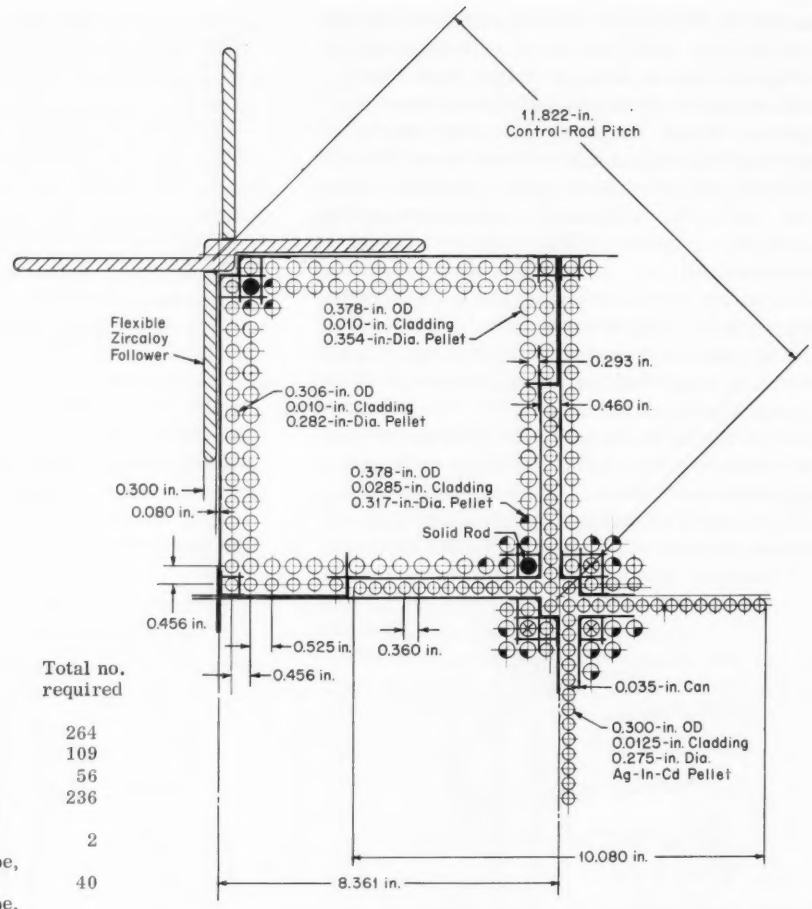

	Total no. required
Fuel assemblies	264
Control-rod slots	109
Tubes per control rod	56
Rods per fuel assembly	236
●, solid stainless-steel corner rods	2
○, 0.306-in.-OD fuel tube, 0.010-in. cladding	40
◕, 0.378-in.-OD fuel tube, 0.0285-in. cladding	8
○, 0.378-in.-OD fuel tube, 0.010-in. cladding	186

Fig. V-2 A cross section of the fuel assembly and control rod.[1]

fuel assembly consists of fuel rods reduced in outside diameter from the normal 0.378 in. to 0.306 in. In addition, two corner rods of each assembly in the vicinity of the greatest flux peaking were replaced by solid-steel rods, and thick cladding was used on eight fuel rods in selected high-power-density positions so that the fuel-pellet area was reduced to 80% of the normal area. All the fuel rods within an assembly have the same enrichment. The assortment of fuel-rod sizes was not needed in the alternate core that used full-length control-rod followers since the water gap producing high peaking factors in the adjacent fuel elements was greatly reduced. The alternate core has the same active fuel length and equivalent diameter as the reference core.

The individual fuel rods are held mechanically within the fuel assembly by a method generally similar to that being developed for the Round 3A plants. Support for the fuel rods is provided by a grid-clip assembly. Rows of clips are interlocked, as in an eggcrate design, and are furnace brazed to form the grid. The grids are welded to a boxlike structure that forms the exterior of the fuel assembly. The structure is perforated to minimize the amount of steel in the system and to allow coolant flow between adjacent assemblies. Fuel rods are inserted through the grids and are held in place by clips or fingers extending from the grid pieces. The clip support is lateral only, and the rods are free to expand axially between the end plates. The end plates and nozzles are

welded to the unit after all the fuel rods are inserted to complete the fuel assembly.

Figure V-3 shows the core cross section. The core contains 264 identical fuel assemblies and 109 individually driven cruciform control rods. The rod pattern is such that every internal fuel assembly has a rod centered adjacent to each of two corners on the diagonal of the assembly. The absorber section is fabricated from 0.275-in.-diameter rods of 80-15-5 silver-indium-cadmium alloy inserted into stainless-steel tubes. The tubes are welded together to form a cruciform, as shown in Fig. V-2. Zircaloy followers are attached to the bottom of the absorber section. In the reference core the follower is 3.7 ft long. In the alternate core the length of the follower is equal to the full core length of 11 ft. The function of the short follower in the reference core is to reduce bypass flow in the control-rod slot and to promote flow mixing between the fuel assemblies.

The nuclear design of the core is tied intimately to the intended method of fuel management because of the large size and high fuel burnup. The fuel loading is 125 metric tons of uranium. The average burnup for the equilibrium core is 24,000 Mwd per metric ton of uranium. This corresponds to a core life of 22,370 EFPH (effective full-power hours) or about 7,460 hr per refueling cycle and results in a refueling period of 12.7 months on the basis of an 0.80 plant factor.

The Westinghouse workers studied[2] several methods of cycling the fuel assemblies in the core. Their purpose was to determine a suitable means of achieving the lifetime requirements while holding the maximum-to-average radial power-density ratio to the limit of 1.5, which is required before the design thermal output can be reached. As is usually the case for reactors of large size and high burnup, the regionwise out-to-in cycling methods were relatively unattractive. The results of the survey of various refueling methods are summarized in Table V-2. The uniform-batch core was calculated for comparison only. Both the 3-region–3-cycle and 5-region–5-cycle shuffles failed to meet either the burnup with the selected feed enrichment or the power-distribution requirements. The 3-region 3-1-2 shuffle, in which fresh fuel assemblies are inserted in the intermediate region, was tried since the results of the out-in cycle studies indicated that the coupling between fresh and burned fuel must be increased to obtain higher burnup and satisfactory power distribution. The trial was unsuccessful, and it was concluded that, whenever a sizable fraction of a large core is replaced by fresh fuel, a large power peak always occurs in that region, and the remainder of the core serves as a multiplying reflector. The method of fuel management proposed, which avoids regionwise cycling, is designated "Roundelay multibatch." In the equilibrium cycle fresh elements are inserted in a uniform

Table V-2 CHARACTERISTICS OF DIFFERENT REFUELING METHODS FOR A 1000-MW(e) PRESSURIZED WATER REACTOR[2]

(Feed Enrichment Is 3.4 Wt.% in All Cases)

Refueling method*	Discharge burnup	Burnup/ batch burnup	Power ratio $P_{max,(radial)}/P_{av.}$	$K_{initial}$ (no Xe)
Uniform batch	15,250	1.00	1.99	1.229
Out-in				
3 region–3 cycle	20,440	1.34	1.96	1.126
5 region–5 cycle	21,960	1.44	1.92	1.095
3-region 3-1-2	21,740	1.43	2.28	1.158
Roundelay 3-batch	23,290	1.53	1.35†	1.116
Roundelay 5-batch	25,830	1.69	1.22†	1.081

*In the out-in refueling method, fresh fuel is fed to the outermost of several concentric fuel regions and subsequently moved inward at each refueling cycle. Spent fuel is removed from the innermost region. The 3-region 3-1-2 method is a variation in which fresh fuel is loaded into the intermediate region of a 3-region core. The numbering sequence taken in inverse order identifies the region in which the fuel is successively placed, the regions being numbered from out to in. In the Roundelay method the core is divided into a large number of adjacent regions, each of which has a number of fuel batches (usually one assembly is a batch). At every refueling cycle a spent fuel batch is removed and replaced by a fresh batch in each region. The partially spent fuel is never moved.

†These values do not include local "ripple" effects.

distribution throughout the core at each refueling operation. For example, with Roundelay 3-batch, every third element is replaced, and the other elements are left in place. In Fig. V-3 the fuel assemblies are numbered in the order

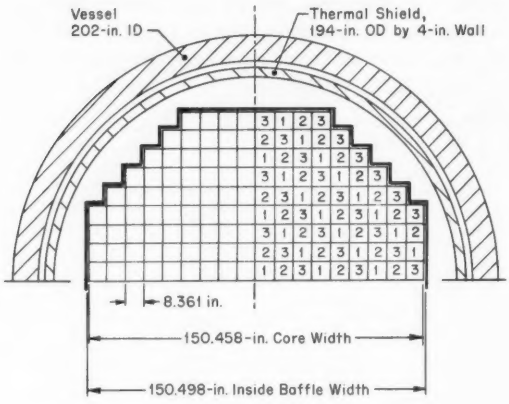

Fig. V-3 Cross section of vessel core.[1]

in which they might be replaced in the reference core; during one refueling all No. 1 fuel assemblies would be replaced, and so on. It was found that the mixing of the fresh and burned fuel assemblies produces strong coupling between them and permits improved power production from the burned elements. The improved burnup is evident in the results shown in Table V-2. The favorable values of maximum-to-average power ratio are illusory, however, since the survey study did not take into consideration the "ripple" on the overall power distribution resulting from significantly different power production from adjacent fuel assemblies with greatly different burnup. As a result the reference core failed to meet the design criteria, although two changes were proposed to permit it to do so, as follows.

1. Reduce the local power ripple by increasing the number of fuel assemblies. A 673-fuel-assembly core with a 10-by-10 fuel-rod array showed a much improved power distribution.

2. Select a core array that has a center fuel assembly so that the replacement of the central group of four elements forced by symmetry would be eliminated. A very poor power distribution results from the power spike produced when the four fuel assemblies adjacent to the center are replaced together.

With Roundelay 3-batch refueling, it was found that after six refueling steps the core conditions are essentially those of the equilibrium cycle.

The thermal and hydraulic characteristics for both the reference and alternate cores are presented in Table V-3. A review of these parameters gives the best insight into the methods by which the rather remarkable power density of 80 kw/liter is expected to be achieved in these very large cores. No single item makes a large contribution to improved performance, but a substantial improvement is expected from a combination of many small items, with careful attention to their detailed interaction. This attention to detail extends not only to the physical arrangements of core components (e.g., the array of different type fuel rods within one assembly) and to a more uniform approach to design limitations over the core volume (e.g., promoting interchannel mixing to reduce enthalpy-rise hot-channel factors) but also to a reexamination of the limitations themselves. For example, the design limitation of a DNB (departure from nucleate boiling) ratio of 1.25 at 115% of full power represents less margin than is used in current practice. Evidently the belief is that operational experience from present-day plants plus adequate in-core instrumentation will permit satisfactory operation within these margins.

The composition of F_q, the ratio of maximum heat flux to average heat flux in the core, used for design purposes, is[1]

Subfactor	F_q
Axial	1.60
Radial	1.50
Local power peaking	1.30
Transient hot-channel factor	1.02
Engineering	1.045
Design overall factor	3.33

For $F_{\Delta H}$, the ratio of maximum coolant enthalpy rise to average coolant enthalpy rise over the total length of the core, the composition is[1]

Subfactor	$F_{\Delta H}$
Radial	1.5
Transient factor	1.02
Engineering	
Net hot cell	1.07
Uncertainty	1.03
Flow distribution	1.07
Design value total	1.8

Table V-3 THERMAL AND HYDRAULIC CHARACTERISTICS OF THE CORE[1]

	Reference design (short followers)	Alternate design (full-length followers)
Total heat output		
Mw	3220	3220
Btu/hr	10.99×10^9	10.99×10^9
Heat generated in fuel, %	97.4	97.4
System pressure, nominal psia	2050	2050
Hot channel factors in steady-state		
Heat flux, F_q	3.33	2.94
Enthalpy rise, $F_{\Delta H}$	1.80	1.80
Coolant conditions		
Total flow rate, lb/hr	160.0×10^6	160.0×10^6
Effective flow rate for heat-transfer, lb/hr	144.0×10^6	144.0×10^6
Flow area for heat-transfer flow (unit cells), sq ft	69.77	68.2
Average velocity along fuel rods, ft/sec	12.7	13.0
Average mass velocity along fuel rods, lb/(hr)(sq ft)	2.06×10^6	2.11×10^6
Coolant temperature, °F		
Nominal inlet	546	546
Maximum inlet due to instrumentation error and dead band	550	550
Average rise in vessel	52	52
Average rise in core	57	57
Average in vessel	572	572
Average in core	574.5	574.5
Nominal outlet of hot channel	639	639
Maximum outlet quality of hot channel, wt.%	2.0	2.0
Maximum outlet enthalpy of hot channel, Btu/lb	687	687
Saturation enthalpy at minimum steady-state pressure, Btu/lb	675	675
Average film coefficient, Btu/(hr)(sq ft)(°F)	4850	5040
Average film-temperature difference, °F	34	30
Heat transfer		
"Active" heat-transfer surface, sq ft	65.5×10^3	70.9×10^3
Average heat flux, Btu/(hr)(sq ft)	163.5×10^3	151.0×10^3
Maximum heat flux, Btu/(hr)(sq ft)	544.3×10^3	444.0×10^3
Maximum thermal output, kw/ft	16	13.2
Average fuel temperature in core, °F	1535	1537
Heat transfer (continued)		
Maximum rod-surface temperature at nominal pressure, °F	645	645
DNB ratios*		
Average q''-DNBR at 100% power at 2050 psia	1.51	1.76
Average q''-DNBR at 115% power at 2200 psia	1.39	1.62
H-DNBR at 100% power at 2050 psia	1.49	1.53
H-DNBR at 115% power at 2200 psia	1.23	1.26

	Normal rod	Small rod	
Fuel rod (cold dimensions)			
Outside diameter, in.	0.378	0.320	0.3884
Cladding thickness, in.	0.010†	0.010	0.0152
Diametral gap, in.	0.004	0.004	0.004
Pellet diameter, in.	0.354†	0.296	0.354
Density of UO_2, % of theoretical density	96.5	96.5	96.5
Fuel length (pellets only), in.	132	132	132
Pitch, in.	0.525	0.456	0.523
Rod array in assembly	16 × 16		16 × 16
Rod per assembly	194	40	240
Total number fuel rods in assemblies	51,216	10,560	63,360
Hydraulic equivalent diameter of unit cell, ft	0.0469		0.0424
Additional water gap at edge of assembly, in.	0.0305	0.029	0.0305
Control rod			
Number of slots	109		109
General			
Total core area (inside core baffle), sq ft	128.2		133.9
Equivalent core diameter, ft	12.8		13.1
Maximum diameter of core, in.	166.0		169.3
Core length, between fuel ends, ft	11.0		11.0
Length-to-diameter ratio of core	0.86		0.84
Water-to-uranium ratio, unit cell	3.29		3.12
Fuel weight, lb of UO_2	289.3×10^3		314.8×10^3
Pressure drop, psi			
Across core	36		46
Across vessel, including nozzles	51		57
Core power density			
Kw/liter of core	80.7		77.2
Kw/kg of U	27.8		25.6

*The DNB ratios are based on the correlations presented in Ref. 20 and are minimum ratios, within the core, of the DNB condition to the actual condition. The heat-flux DNB ratio, q''-DNBR, applies to the subcooled regions of the core. The enthalpy-rise DNB ratio, H-DNBR, applies to quality regions of the core.

†Eight rods have a 0.0285-in. cladding thickness and a 0.317-in. pellet diameter.

In both tabulations above the transient factor provides for rod motion required for a 5% step change in load at 95% power level. It is expected that coolant mixing within the core, both between channels and between fuel assemblies, will be required to achieve the $F_{\Delta H}$ design value. Provision has been made in the core to promote mixing. Flow mixing is promoted between fuel assemblies to cool the channels at the assembly edge, where the power peaks, by mixing vanes installed on the grids within the upper 5 ft of the core and by staggering the grids in this region. Bulk boiling at the exit of the hot channel is permitted, to the extent of 2 wt.% quality, to keep the coolant-flow requirements within the capabilities of a seven-loop primary system.

In a study associated with the 1000-Mw(e) pressurized-water-reactor (PWR) design, the effects of core height, enthalpy rise, and burnup on the axial power distribution were investigated. The following quotation from Ref. 2 states the general problem:

> In designing very large reactor cores, it is important to understand the dependence of power distribution on core height, enthalpy rise, and burnup. To illustrate this point, consider the following hypothetical situation. Suppose a reactor with a core height of 10 feet has been designed to produce a given power output. If a new reactor design is required which has a 10% higher output, one might propose an increase in the core height to 11 feet, maintaining the same average power density. However, the axial hot channel factor might be greater in the 11 ft. core; if the increase in hot channel factor is 10%, the power capability is not increased at all in going from a 10 ft. to an 11 ft. core, assuming a burnout heat flux limitation. The power distribution might be expected to become worse as the enthalpy rise is increased since the water density becomes more non-uniform.

The conclusions (Ref. 2) drawn as a result of the study were as follows:

> 1. In the first core, which contains only fresh fuel, the axial peaking increases slightly with core size. At a burnup of a few thousand MWD/MTU, there is little variation in peaking factor with core size. Beyond 3000 MWD/MTU, the larger cores may have slightly less axial peaking than smaller cores.
> 2. In a cycle typical of equilibrium, the peaking factor appears to increase substantially with core size; however, burnup effects have reduced the equilibrium peaking factor to a low value in all cases so that the peaking is not serious, even in the larger cores.
> 3. All steady state power distributions which were studied had axial peaking factors less than 1.60, which is the design value for the 1000 MWe PWR.

Reactivity control of the reactor is provided by a combination of the mechanically actuated neutron-absorbing control rods and a chemical neutron poison dissolved in the reactor coolant. The soluble poison is boron in the form of boric acid. Rapid reactivity changes resulting from rapid load changes, safety shutdown, Doppler, and other rapid transient effects are controlled by the rods. The slower acting reactivity changes due to fuel depletion, samarium, xenon, and gross temperature effects are accommodated by adjusting the concentration of the neutron poison in the primary coolant. The principal advantages in using a soluble poison are the improved core power distribution resulting from being able to withdraw most of the control rods during operation and the reduced total reactivity compensation required of the control rods since they are no longer required to shut down the reactor to the cold clean condition by themselves. The principal disadvantages are the large volume of primary coolant that must be handled when bleed-and-feed dilution is used to reduce the boron concentration and the influence of the poison in reducing the moderator coefficient of reactivity or even causing it to change sign. In connection with the latter point, the criteria for the reference design permit the moderator coefficient of reactivity to vary from positive to negative during core life. It is proposed that the stability of the reactor be preserved through the combination of the Doppler effect and the coolant temperature controller.

The estimated boron concentrations for the first and equilibrium core cycles are[1]

Condition	Boron concentration, ppm	
	1st cycle	Equilibrium
Refueling shutdown; rods in; $k = 0.90$	3880	2930
Cold normal shutdown; rods in; $k = 0.97$	2880	1960
Hot normal shutdown; rods in; $k = 0.97$	2670	1550
Hot full power; no rods; no poison	2780	1810
Hot full power; no rods; Xe poison	2310	1370
Hot full power; no rods; Xe and Sm	2150	1240
End of life	≈ 0	≈ 0

In recent operation the Yankee Atomic Electric Co. reactor at Rowe, Mass., has been successfully employing soluble-poison shim

control, and other reactors have run in this manner on an experimental basis. The degree to which the soluble poison is employed in the reference large PWR, however, is significantly greater than in systems that have been run to date.

With the heavy dependence on soluble shim control, it might seem that the reference design employs an unusually large number of control rods (109). The large number results from uncertainties regarding spatial instabilities in the large core, which might conceivably arise from either sustained xenon oscillations or Doppler oscillations. The possibility of both was studied. It was found that for the conditions normally existing in a PWR, i.e., negative Doppler coefficient, no Doppler oscillations are possible, even for a very large reactor. In regard to xenon oscillation, the conclusions were not as definite and were summarized in Ref. 2 as follows:

> 1. The nominal temperature coefficient is sufficiently negative to prevent sustained Xe oscillations of constant or increasing amplitude, even with pessimistic assumptions for the degree of flux flattening.
> 2. With the minimum temperature coefficient and a pessimistic degree of flux flattening, the calculations predict the 1000 MWe core is near the threshold for sustained oscillations.
> 3. Damped oscillations are predicted in all directions for both the nominal and minimum temperature coefficients. Damped oscillations do not represent a serious operational problem if the degree of damping is sufficient to quickly reduce the amplitude of the oscillation. With the nominal temperature coefficient, the damping is probably sufficient to prevent any serious problem; however, with the minimum coefficient, very little damping is expected and operational problems could occur. These conclusions must be qualified since no definite standards have been established regarding the degree of damping required for satisfactory reactor operation. . . .

It is further stated in Ref. 2 that the possibility of xenon oscillations is not believed to be a feasibility problem of the 1000-Mw(e) PWR since reactors have been operated in the presence of such oscillations.

In-core instrumentation is proposed to detect nuclear flux tilts as well as to monitor reactor-coolant temperatures. Neutron fluxes at selected locations in each of the 66 fuel assemblies in one quadrant of the core and at 3 positions in each of the remaining quadrants would be measured by miniature in-core neutron detectors. Temperatures at the outlets of each of the 66 fuel assemblies in one quadrant of the core and at 34 selected positions in the other three quadrants would be measured by sheathed Chromel-Alumel thermocouples.

A second alternate core design aimed principally at an improvement in control-rod features was proposed, although a complete core design was not developed in the study (Ref. 1). This alternate is based on replacing the separate cruciform control rods by a cluster of poison elements arranged in one or more rings and located within the fuel assembly instead of between the fuel assemblies. The individual poison elements are approximately the size of the fuel tubes and move in thimbles located within the fuel assembly. This "rod-cluster-control" (RCC) concept eliminates the necessity for followers and makes the use of canless fuel assemblies more attractive. A model of the rod-cluster-control assembly is shown in Fig. V-4. The RCC fuel assembly requires no change in the basic fuel lattice, and the spring-clip grids for holding the fuel rods in the lattice are retained. The guide tubes in which the individual control elements move are permanently fixed within the lattice of the fuel assembly. The individual control elements are fastened together above the fuel assembly by means of a spider, as shown in Fig. V-5, and all elements within an assembly move up and down together. The guide tubes within the fuel assembly are perforated over a substantial length to provide for coolant flow. The venting is controlled at the bottom of the tube to serve as a dashpot during scramming of the control element. The rod-cluster control-guide tube is shown in Fig. V-6. Advantages of the rod-cluster control are summarized in Ref. 1:

> 1. Improved power distribution due to (a) separation of interassembly peaking from control slot peaking and (b) breakup of control slot peaking by distributing the control material as individual rods throughout the lattice.
> 2. More control per weight of absorber provided the most favorable geometry can be selected.
> 3. More uniform distribution of control. This will result in better power distribution control in the event of unstable power distribution and better temperature and pressure dead-band control because of the lower worth per rod step.
> 4. Less parasitic absorption if elimination of the stainless steel can is successful which will improve the fuel cycle costs.
> 5. Complete elimination of followers.
> 6. Reduced coolant bypass flow.
> 7. Simplification in mechanical design.

Although rod-cluster control is considered only as an alternative in the 1000-Mw(e) PWR

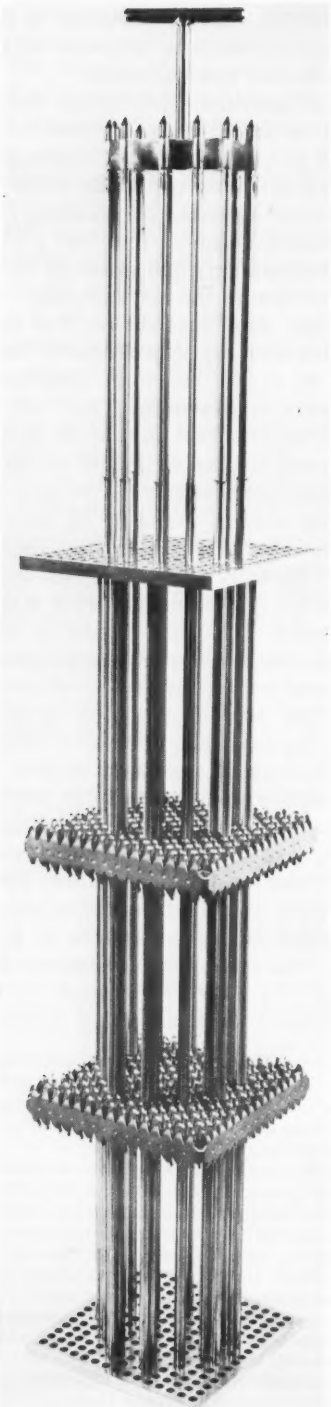

Fig. V-4 Fuel-assembly model for rod-cluster control.[1]

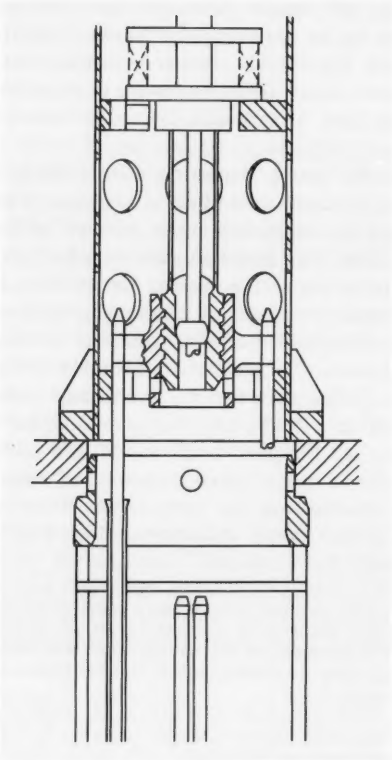

Fig. V-5 Coupling for rod-cluster control.[1]

study, significant development has been devoted to the concept, and it has been incorporated in the design of the San Onofre reactor (Ref. 15). Rod-cluster control could reasonably be expected to be adopted for the Connecticut Yankee and Malibu reactors also.

As mentioned earlier in this review, this 1000-Mw(e) Closed Cycle Water Reactor Study should rest on firmer ground than the usual run of reactor-feasibility studies because it is based on information generated under the massive LRD Program being conducted for the San Onofre reactor. References 4 to 15 are progress reports on this program. Topical reports, Refs. 16 to 39, on the same program treat the reactor subjects covered in the 1000-Mw(e) study (Refs. 1 and 2) in greater depth and are keyed, of course, to the San Onofre reactor. For example, a number of mechanically assembled fuel assemblies have been irradiated in the Saxton reactor, and additional assemblies have been prepared for irradiation. These included two rod-cluster-control assemblies, one a 3-

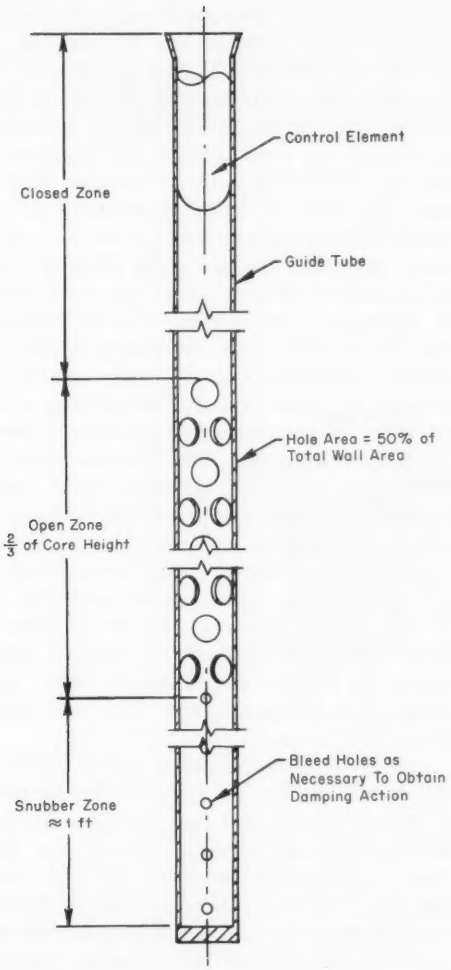

Fig. V-6 Guide tube for rod-cluster control.[1]

by-3 and the other a 9-by-9 array. Fuel cladding of these assemblies included both thin-walled stainless steel and Zircaloy.

A general comment appears appropriate on the size of components for large pressurized-water reactors. At the time this 1000-Mw(e) PWR study was conducted, a 1000-Mw(e) power level was believed to be the highest achievable from a single reactor vessel in the relatively near future. Similarly, seven coolant loops were required because of restrictions on the maximum size of steam generators and main coolant pumps. Recent indications are that manufacturers are now capable of providing these key components in higher unit ratings. As previously mentioned, pressure vessels for 1500-Mw(e) units appear to be feasible.[3] Steam generators of almost twice the capacity used in the study are being discussed. If coolant pumps are not restricted to canned-motor units, the remaining restriction would be only the size of volute that can be cast. This would permit pumps of increased capacity.

EBWR

Operation of the Experimental Boiling Water Reactor (EBWR) at power levels up to and including 100 Mw(t) has been previously reviewed in *Power Reactor Technology*, 7(3): 317-320, on the basis of several topical reports. Reference 40 contains a collection of the detailed test reports that cover operation since the modification of the reactor and plant for the higher power up through operation for brief periods at 100 Mw(t). The test reports contain detailed accounts of the loading sequence and initial critical testing. Physics tests included critical control-rod-position determination, rod calibrations, and measurements of temperature and void coefficients and flux distribution. The response of the reactor to step reactivity changes was determined with reactor periods ranging from 15 to 40 sec and peak power levels near 1 Mw(t). Analytical correlation of the peak power and energy production during these transients with the reactor period was obtained using an energy-production-dependent reactivity feedback. Inspection of the control rods irradiated during prior operation of the EBWR is described, including metallurgical and radiochemical examinations. Thermal and hydraulic testing included temperature measurements in the reactor, determination of recirculation rate, measurements of steam-volume fractions in the core and riser, as well as investigation of steam carry-under and moisture carry-over.

Design Studies of a 1000-Mw(e) Fast Reactor

Four independent design studies (Refs. 41 to 44) were made for the AEC on a 1000-Mw(e) ceramic-fueled fast breeder reactor cooled with liquid sodium. In two of the studies the fuel was UO_2-PuO_2, whereas in the other two studies UC-PuC was used. These studies, which were focused on the reactor and primary heat-

removal systems, represent the first phase in AEC's program to develop basic fast breeder concepts for large commercial power stations. The objectives in the studies were to develop designs that optimized fuel-cycle costs, obtained attractive fuel-doubling times, and permitted high-temperature steam conditions at the turbine, consistent with safety requirements in fast reactors. The studies thus included core physics and thermal-hydraulic analysis, mechanical design features, fuel-handling concepts, and fuel-cycle economics. The following ground rules were common to all studies:

1. The performance was to be evaluated for equilibrium cores.

2. The fuel cladding was to be a stainless steel.

3. The primary sodium temperature was to be sufficiently high to produce 1000°F steam, taking into account the temperature drop in the intermediate heat exchanger.

4. The breeding ratio was to be greater than 1.2, with a reasonable doubling time.

5. The fuel was to be considered government owned with a 4¾% rental charge.

6. The value of $10 per gram was to be used for ^{239}Pu and ^{241}Pu in the form of the nitrate.

7. The feed material to the plant for the equilibrium core was to be depleted uranium containing 0.3 wt.% ^{235}U.

In a recent feature article by Okrent[45] in *Power Reactor Technology*, various problems were discussed which affect the performance of large sodium-cooled ceramic-fueled fast reactors. In general, the considerations introduced by economics, breeding, and safety give rise to conflicting requirements in optimizing the design of such reactors. A ceramic fuel after exposure in the reactor cannot be considered to provide the reliable axial thermal expansion that, in smaller metal-fueled reactors, is responsible for a significant rapidly acting negative reactivity coefficient. On the other hand, the presence of oxygen or carbon in the ceramic softens the neutron spectrum so that a sizable negative Doppler coefficient of reactivity can be obtained. The change in reactivity upon loss of sodium from the core becomes more positive with increasing reactor size because the positive reactivity effects associated with changes in neutron spectrum become more important relative to the negative neutron-leakage effect. The buildup of ^{240}Pu and fission products in the equilibrium core increases the positive reactivity effects due to sodium voiding, as would also the substitution of niobium for steel structures. Any measure that increases the neutron leakage from the core also tends to shift the sodium void coefficient in the negative direction for two reasons. First, the increase makes the effect of sodium on the neutron leakage more important. Second, an increase in the concentration of fissile isotope is required; this, therefore, results in a harder spectrum that is less sensitive to changes in sodium density. The higher leakage has other, unattractive consequences: if brought about by a thinning of the breeder blanket, it decreases the total breeding ratio, and, if brought about by the use of high-leakage core geometry, it decreases the internal breeding ratio and increases the rate of reactivity loss with fuel burnup. The Doppler reactivity coefficient can be improved by the addition of a fixed moderator to the core, such as BeO, to soften the neutron spectrum; however, this is detrimental to the breeding ratio and doubling time.

Among the other problems that required consideration in these studies were the limitations of the stainless-steel fuel cladding at the high temperature required to obtain the 1000°F steam temperature specified for high thermodynamic efficiency, the utilization of the fuel at high burnup and high heat ratings for attractive fuel-cycle economics, thermal-stress problems in the reactor vessel and primary system imposed by high-velocity sodium operating at temperature differences in the range of 200 to 300°F, and reliable methods of refueling without excessive reactor downtime.

The four fast reactor design studies were evaluated by the AEC[46] with the assistance of the Argonne National Laboratory and the Los Alamos Scientific Laboratory. A very brief summary description of the four reactor concepts was presented in a paper by Koch et al.[47] A summary of the nuclear and safety characteristics of the reactor concepts was compiled by Okrent et al.,[48] and the fuel-cycle economics were evaluated by Link et al.[49] A paper by Klotz and Miller described the Allis-Chalmers design.[50]

A brief description is given below of the four 1000-Mw(e) concepts. The core arrange-

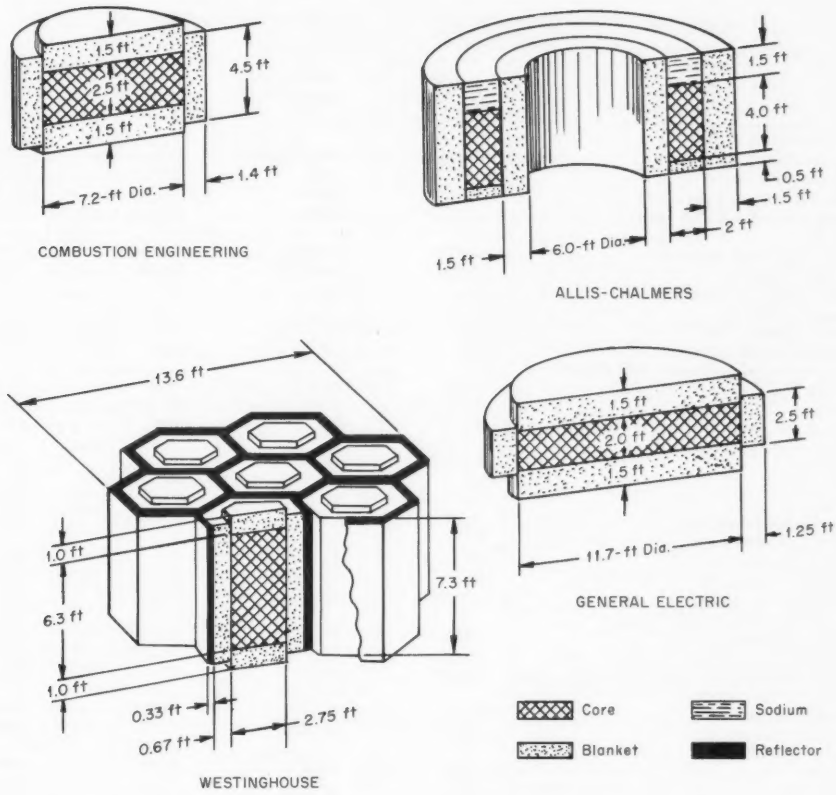

Fig. V-7 Reactor-core arrangements for four 1000-Mw(e) design studies.

ments are shown diagrammatically in Fig. V-7, and the major characteristics of the four concepts are presented in Table V-4.

Allis-Chalmers Reactor Concept

To reduce the sodium void coefficient as much as possible, this concept uses a thin annular core having high neutron leakage. The core annulus is 2 ft thick, 13 ft in outside diameter, and 9 ft in inside diameter, with a volume of 7720 liters. The sodium void coefficient is decreased even further because no breeder blanket is used above the core region; instead a sodium space is provided at the top of the core with a layer of B_4C above the sodium. The fuel pins contain UO_2-PuO_2 pellets that are distributed axially in 3-in. compartments within the pins to minimize reactivity effects from fuel compaction. The fuel pellets have hollow centers to permit a maximum heat rating of 13 kw/ft with a cladding temperature of 1420°F. There are 123 fuel pins in the hexagonal fuel assembly which are held in place by six grids, 12 in. apart, along the length of the assembly, with tie rods at alternate corners of the assembly. The fuel assemblies are held down hydraulically and are individually orificed to obtain a uniform sodium exit temperature. Heat is removed from the 1200°F primary sodium by means of six external loops.

For refueling the fuel elements are located by double rotating and indexing shield plugs. After the reactor is cooled to 350°F and the sodium level is lowered, direct visual observation of the core is possible for grappling the fuel elements. The fuel is removed to an argon-cooled cask, is cleaned with steam to remove the sodium, and is then transferred to an on-site reprocessing plant. The blanket is shuffled in an out-in manner to match the orificed sodium flow with the power generation in the elements. This avoids large changes in exit sodium temperature in the blanket assemblies

Table V-4 CHARACTERISTICS OF THE 1000-Mw(e) CERAMIC-FUELED FAST REACTOR CONCEPT

	Allis-Chalmers[41]	Combustion Engineering[42]	General Electric[43]	Westinghouse[44]
Core and blanket				
Core geometry	Annulus	Flat cylinder	Flat cylinder	7 modules
Core volume, liters	7520	2895	6030	7050
Axial blanket volume, liters	960	3500	9050	2400#
Radial blanket volume, liters	17,700	4800	4200	19,850
Fuel form				
Core and axial blanket	Oxide	Carbide	Oxide	Carbide
Radial blanket	Oxide	Carbide	Oxide	Oxide
Active height of core, ft	4	2.5	2.0	6.3
Blanket thickness				
Axial blanket, ft	0.5	1.5	1.5	1.0
Radial blanket, ft	1.5	1.4	1.3	0.7
Composition of core and axial blanket				
Fuel, %	29.4	25.6	34.8*	29.4†
Sodium, %	40	66.5	46.4	55.1
Steel, %	30.6	7.9	18.8	15.5
Composition of radial blanket				
Fuel, %	55	45	50.7	55
Sodium, %	30	43	32.1	25
Steel, %	15	12	17.2	20
Core fissile metal, kg	3690	1155	2304	3686
Blanket fissile metal				
Axial blanket, kg	6	32	58	23
Radial blanket, kg	260	83	80	171
Core load (metal), kg	17,760	8913	12,828	23,420
Blanket loading (metal)				
Axial blanket, kg	2210	10,696	19,242	7800
Radial blanket, kg	84,566	27,886	24,300	56,886
Core load (ceramic), kg	20,200	9400	14,600	25,200
Blanket loading (ceramic)				
Axial blanket, kg	2510	11,250	21,900	8200
Radial blanket, kg	96,100	29,400	27,500	59,800
Power, Mw(t)				
Total	2500	2500	2500	2500
Core	2125‡	1950	2125	2170
Axial blanket		200	300	35
Radial blanket	375	350	75	295
General				
Core irradiation level, Mwd/metric ton of U	100,000	110,000	110,000	100,000
Breeding ratio§	1.32	1.42	1.25	1.57
Doubling time,§ years	19.5	6.2	15.8	11.7
Sodium void worth¶ (100% core voided), $\%\Delta k$	0.0	1.0	0.4	0.3
Doppler coefficient, $-T(dk)/(dT) \times 10^{+3}$	2.6	5	5	12
Fuel-cycle cost,§ mills/kw-hr	0.69	0.30	0.57	0.28
Size, ft				
Reactor diameter	16.0	10.0	14.2	13.6
Reactor height	6.0	5.5	5.0	8.3
Vessel diameter	20.0	16.5	18.0	18.0
Vessel height	25.0	40.7	33.0	36.0
Thermal parameters				
Specific power, kw/kg				
Core U + Pu ceramic material§	100	198	150	86
Core fissile material¶	640	1680	920	520
Power density in core,§ Kw(t)/liter	282	695	365	308
Temperature, °F				
Core inlet	950	850	800	979
Cladding peak	1330	1400	1332	1400
Fuel peak	4615	2600	4700	2184
Core outlet	1200	1120	1100	1200
Fuel bond	Helium	Sodium	Helium	Sodium
Coolant				
Sodium flow, $(lb/hr) \times 10^{-6}$	114	113.6	95.4	128
Core velocity, ft/sec	10	20	11.1	26.5
Loop pressure drop, psi	90	59.8	40	113

Table V-4 (Continued)

	Allis-Chalmers[41]	Combustion Engineering[42]	General Electric[43]	Westinghouse[44]
Fuel				
Fuel-pin-cladding outside diameter, in.				
Core and axial blanket	0.30	0.30	0.25	0.30
Radial blanket	0.607	0.45	0.50	0.464
Cladding thickness, in.				
Core and axial blanket	0.028	0.011	0.015	0.010
Radial blanket	0.015	0.016	0.020	0.020
Sodium-bond gap, in.				
Core and axial blanket		0.010		0.006
Radial blanket		0.011		
Pellet outside diameter, in.				
Core and axial blanket	0.24	0.259	0.22	0.268
Radial blanket	0.574	0.396	0.45	0.420
Pellet, inside diameter, in.	0.10		0.06**	
Active core height, in.	48	30	24	75
Active blanket height, in.				
Axial blanket	6	36	36	24
Radial blanket	72	54	36 and 60	87
Assemblies				
Distance across flats, in.	4.45	6.241	8.75	5.104
Triangular pitch of pins, in.				
Core and axial blanket	0.375	0.468	0.338	0.426
Radial blanket	0.69	0.539	0.565	0.496
No. of pins per assembly				
Core and axial blanket	123	169	470	120
Radial blanket	37	127	208	91
No. of assemblies in region				
Core and axial blanket	498	157	225	252
Radial blanket	858	156	108	357
Total no. of pins in region				
Core and axial blanket	61,254	26,533	105,750	30,240
Radial blanket	31,709	19,812	22,464	19,812
Feed enrichment, average, %				
Core	20.8	13.0††	18.0††	15.7
Blankets	0.3	0.3	0.3	0.3

*Includes BeO.
†Includes cermet.
‡Includes bottom axial blanket.
§Per contractor calculations.
¶Per evaluator calculations.
**Formed during operation.
††Zoned.

with the rapid buildup of plutonium associated with the high radial neutron leakage from the core.

Combustion Engineering Reactor Concept

This concept uses a conventional cylindrical core that has a volume of 2895 liters. The core is 2.5 ft high and is 7.2 ft in diameter, with a length-to-diameter ratio of 0.35. The carbide fuel is sodium bonded to the 11-mil-thick cladding made of type 19-9 DL stainless steel. The sodium bond permits higher heat fluxes for a given maximum temperature limit on the fuel and also accommodates the swelling of the fuel with burnup. The top and bottom axial blankets are integral with the core. A 15-in. gas space is provided on top of the upper axial blanket to accommodate a gas release of 11% over the 100,000 Mwd/ton exposure of the element. The carbide is slightly hyperstoichiometric, i.e., carbon content is greater than 4.8 wt.%, to limit swelling and gas release in fuel operating at a maximum temperature of 2600° F. Several methods are proposed to prevent the carburization of the cladding. The hexagonal fuel assemblies in the core each contain 169 fuel pins that are held together by band wraps. The radial blanket is also carbide fuel, with a residence time three times that of the core. Halfway through its life each blanket element is rotated 180° to equalize its exposure and to increase the coolant flow to accommodate the higher heat generation.

For refueling the fuel elements are located by a single rotating and indexing plug and a manipulator arm and are transferred under sodium to an adjacent decay storage pool of sodium. After three months' decay the elements are removed, steam cleaned to remove sodium, and prepared for shipment off-site in a water-cooled cask.

There are six conventional primary loops outside the reactor vessel. The pump is at the outlet to minimize the pressure of the cover gas in the reactor vessel.

Combustion Engineering also presents an advanced design featuring a voided radial gap between the core and blanket to obtain a negative sodium coefficient for complete voiding of the core coolant. The theoretical basis for the gap was described in a recent paper (Ref. 51).

General Electric Reactor Concept

To obtain high neutron leakage from the core, this concept uses a highly "pancaked" core, 2 ft high and 11.7 ft in diameter, which has a volume of 6000 liters. There are three radial zones of fissile plutonium enrichment for power flattening. The maximum heat rating of 22.7 kw/ft is obtained with oxide fuel that has a hollow cored center, formed during initial reactor operation. The maximum temperatures for the fuel and the type 316 stainless-steel cladding are 4700 and 1330°F, respectively. The fuel pins are fastened to a grid in the fuel box by use of a T slot in the lower end plug and a mating bar in the grid. The pins are positioned along their length by means of slotted spacer tubes that contact the three surrounding fuel pins. There is an upper shield-plug section that is integral with the fuel pins so that the fuel elements are held down by their own weight. The core contains 7 vol.% beryllium oxide to increase the magnitude of the Doppler coefficient by softening the neutron spectrum. The entire primary system, including the reactor core, the six heat exchangers, and the six pumps, is immersed in a large tank of sodium, 52 ft in diameter, so that problems associated with sodium leakage and thermal expansion in the primary piping are minimized.

A shielded inert-gas-filled cell with manual manipulators is provided directly over the reactor for refueling. The vessel head is removed and the fuel is transferred under sodium using hot-cell techniques. After they have decayed in a storage tank, the fuel elements are removed and shipped under sodium without any cleaning.

General Electric also presents an advanced core without beryllium oxide to obtain a higher breeding ratio. The fuel burnup in this design is 200,000 Mwd/ton.

Westinghouse Reactor Concept

The reactor consists of seven hexagonal cylindrical modules, each containing a high-leakage core that is 2.75 ft in diameter and 6.3 ft high, with a total core volume of 7000 liters. Each core is surrounded by an 8-in.-thick blanket of UO_2 and a 4-in.-thick layer of graphite that decouple the modules from each other. The fuel consists of pressed and sintered carbide pellets of 90% density; the carbide is hypostoichiometric, carbon content less than 4.8 wt.%, to avoid carburizing the type 316L stainless-steel cladding. The pellets are compartmentalized in the pins to minimize reactivity effects from compaction of the ceramic fuel. The axial blankets containing UC form an integral part of the fuel pins. The maximum temperatures for the fuel and the cladding are 2184°F and 1400°F, respectively. Iron is added to the fuel to combine with the free metallic phase forming $(U\text{-}Pu)Fe_2$. This is to avoid forming in the cladding a plutonium-iron eutectic that has a melting point of only 770°F and also to tie up any free plutonium in the grain boundaries to minimize fuel swelling. The fuel is assembled in what is called a Controlled Fuel-Expansion Assembly to provide a negative reactivity coefficient due to thermal expansion and thus supplement the negative Doppler coefficient. Each ceramic fuel pin is made in two pieces; one piece is attached to the upper assembly plate, and the other is attached to the lower assembly plate. A small gap is left in the center. The size of this gap is controlled by the thermal expansion of seven cermet type fuel pins in each assembly which tie the upper and lower grip plates together. The cermet is 20 vol.% UO_2 in stainless steel with a ^{235}U enrichment of 30%.

The fission-product gases are vented from the fuel pins to the primary sodium coolant to minimize the stresses in the cladding. The fuel assemblies are held down in the reactor by means of a push-pull latching device at the bottom of the assembly.

The reactor vessel is designed with a coaxial arrangement for the inlet-outlet pipes to minimize stresses in the vessel from thermal expansion and to minimize the number of penetrations. As a result of the high neutron leakage into the radial blanket of each module, the plutonium content, and therefore the power generation in the blanket elements, increases

markedly with exposure in the reactor. Hence provision is made for periodic adjustments in the sodium flow to the blanket elements. For refueling the reactor-vessel head is removed, and by hot-cell techniques the fuel is transferred visually, using gas cooling, to an antimony-lead-filled cask for shipping.

Nuclear and Safety Characteristics

All four reactors have neutron lifetimes in the range from 3 to 6 $\times$ 10^{-7} sec, effective delayed-neutron fractions of about 0.004, and sizable negative Doppler coefficients. The power coefficients of reactivity are all negative and in the range from -1 to -3×10^{-6} Δk/Mw. Relatively flat radial power distributions are obtained in the cores with low length-to-diameter ratios (the Combustion Engineering and General Electric cores) by radial zoning of the plutonium concentration. The tall thin cores (the Allis-Chalmers annular core and the Westinghouse modules) have favorable radial power distributions without fuel zoning. A brief description is given below of the distinguishing characteristics of the four concepts, using parameters obtained from the design reports (Refs. 41 to 44). Note that the values differ from those listed in Table V-4 for the cases where the table values are taken from the AEC evaluation report (Ref. 46) (see Table V-5 for comparison).

The *Allis-Chalmers concept* has a breeding ratio of 1.32, giving a doubling time of 20 years for the fuel inventory. The core conversion ratio is 0.52; an excess reactivity of 0.06 Δk is required for the reactivity decrease between partial reloadings of the core when one-third of the fuel is replaced. A major design basis for this concept is minimizing the possibility of large reactivity insertion should the sodium in the reactor boil, even in the absence of a scram. The voiding of all the sodium in the core gives a reactivity increase of 0.002 Δk. If the sodium boiling occurs in such a way that the upper axial sodium gap is also voided, the reactivity decreases. The Doppler effect will compensate for 0.0017 Δk reactivity before all the oxide fuel reaches the melting point. Control in the annular core requires that several control rods be moved as a coordinated unit because of the small coupling between different sections of the core.

In the *Combustion Engineering concept* the breeding ratio is 1.42, and the specific power in the core is 1680 kw per kilogram of fissionable plutonium; the resulting doubling time is seven years. With the core internal conversion ratio of 0.85, the reactivity change with fuel burnup is only 0.0003 Δk per 1000 Mwd/ton. The reactivity increase for complete loss of sodium from the core is 0.024 Δk, whereas the loss of all the sodium from the core and blankets as well gives no reactivity change. It was calculated that the reactor by means of the Doppler effect can safely absorb a step reactivity increase of 1 dollar and 24 cents without any melting of the fuel or boiling of the sodium. The reactor is partially refueled every two and two-thirds months to replace one-eighth of the core elements so that the reactivity to be controlled is only 0.004 Δk or 1 dollar. Also, sources of potential reactivity addition have been similarly limited; the maximum reactivity worth of a control rod is 1 dollar, and the worth of a fuel assembly is 93 cents. In the event of total loss of coolant flow, it is required that the control rods scram to prevent boiling of the core sodium.

A major objective of the *General Electric concept* is the achievement of a large negative Doppler coefficient of reactivity to counteract reactivity increases that would result from voiding the sodium starting at the core center, even for implausible accidents. Enhancement of the Doppler coefficient is even more important for the oxide fuels, which operate at higher temperature than the carbide fuels, since the Doppler coefficient usually decreases with increasing temperature. The beryllium oxide in the core softens the spectrum so that the Doppler coefficient is enhanced; the Doppler effect will compensate for 0.005 Δk reactivity when the fuel is heated from operating temperature to an average temperature of 4700°F. Voiding all the sodium in the core adds 0.008 Δk, with a maximum increase of 0.014 for some configuration of partial voiding.

It has been calculated that a step reactivity increase of 1 dollar and 70 cents will not cause fuel damage or sodium boiling. The blockage of coolant flow in the core at full power will cause boiling to start at the center with a maximum reactivity gain of less than 1 dollar so that the reactor does not become prompt critical. Up to 3 dollars and 50 cents of reactivity can be inserted at a rate postulated for a refueling accident without any sodium boiling in the core. The energy yield on core meltdown,

which inserts reactivity at the rate of 50 dollars/sec, is equivalent to 200 lb of TNT.

In this reactor of softer spectrum, the breeding ratio is 1.25, with an internal conversion ratio of 0.69. The doubling time is 16 years. The core is refueled every 6 months, when one-sixth of the fuel is replaced; 0.33 Δk excess is provided for fuel burnup.

In the *Westinghouse concept* the sodium coefficient for complete voiding of the core sodium has been made very small, -0.001 Δk, by the use of seven small very loosely coupled core modules, each with its own blanket. A partial voiding of the sodium can increase reactivity by 0.0032 Δk, which is below prompt critical. The controlled-expansion fuel elements provide a reactivity coefficient of $-0.75 \times 10^{-5}/°F$, which supplements the Doppler coefficient of $-0.69 \times 10^{-5}/°F$ at operating temperature. The reactivity sharing between the modules reduces the effect of a reactivity insertion in any one module. The coupling in a clean core is only 0.003 Δk, which increases in the equilibrium core to 0.025 Δk as plutonium builds up in the blanket. The monitoring and control of the modular core may require extensive in-core instrumentation.

The breeding ratio is 1.57, the core conversion ratio is 0.54, and the doubling time is 11 years. The reactor is shut down for refueling every 7 months to replace one-sixth of the core. The reactivity decrease between refuelings, because of fuel burnup, is 0.009 Δk.

Physics and Fuel-Cycle Evaluation

In the course of the AEC's evaluation[46] of the four studies, comparative calculations were performed on breeding ratio, Doppler coefficient, and sodium void coefficient, using consistent cross-section data and calculational methods. The fuel-cycle costs were also recomputed for each concept[49] by applying common procedures for estimating the cost of fuel processing, shipping, and fabrication, taking into account such factors as the diameter, length, and cladding thickness of the fuel pins.

Table V-5 PHYSICS AND FUEL-CYCLE EVALUATION

	Allis-Chalmers concept	Combustion Engineering concept	General Electric concept	Westinghouse concept
Reactivity change for complete voiding of core sodium, Δk				
Contractor calculation	0.001	0.024	0.008	−0.001
Evaluator calculation	0	0.010	0.004	0.003
Doppler coefficient, $-T(dk/dT) \times 10^3$				
Contractor calculation	2.9	5	10	12
Evaluator calculation	4.3	5.4	5.4	3.3
Breeding ratio				
Contractor calculation	1.32	1.42	1.25	1.57
Evaluator calculation	1.20	1.41	1.21	1.38
Doubling time, years				
Contractor calculation	18.4	6.9	13.5	13
Evaluator calculation	30	7.2	20	19
Fuel-cycle cost, mills/kw-hr				
Contractor calculation	0.78	0.30	0.57	0.28
Evaluator calculation	0.70	0.43	0.54	0.43

A common burnup of 100,000 Mwd/metric ton was used, as well as a load factor of 80%. The plutonium credits, however, reflect the contractors' estimate of breeding ratio rather than the normalized values obtained in the evaluation. A comparison with the contractors' values is presented in Table V-5. Except for inventory charges that depend on specific power and plutonium credits that depend on breeding ratio, the other components of the fuel-cycle costs in mills per kilowatt-hour are nearly the same for all concepts: fuel fabrication, 0.4; core capitalization, 0.1; shipping, 0.1; and reprocessing, 0.1. Inventory charges are in the range from 0.1 to 0.3 mill/kw-hr and plutonium credits, based on the normalized breeding ratios, are in the range from 0.2 to 0.4. The Allis-Chalmers study proposes that the fuel be reprocessed on the reactor site. This would lower the fuel-cycle cost for that reactor in Table V-5 by 0.1 mill/kw-hr.

The differences between the contractors' values and those calculated by the AEC evaluators are to some extent indicative of the state of the art in the physics of large fast reactors. Several conclusions are drawn in the AEC evaluation of the four 1000-Mw(e) fast breeder reactors. It is stated in the evaluation that each of the four concepts could be used as the basis of a technically feasible design. A choice cannot yet be made between the mixed-carbide and mixed-oxide fuels because the potential advantages of the carbides depend on information yet to be obtained in development programs. Additional work that should be done prior to committing a 1000-Mw(e) ceramic-fueled fast breeder is outlined in the evaluation. Included are further preliminary designs and optimizations covering the entire plant, safety studies to establish criteria and to predict the course of accidents, physics studies to include cross-section measurements and integral experiments, fuel and materials development, and fuel-handling development.

References

1. Westinghouse Electric Corp., Atomic Power Division, 1000-Mw(e) Closed Cycle Water Reactor Study, Vol. I, USAEC Report WCAP-2385, March 1963.
2. Westinghouse Electric Corp., Atomic Power Division, 1000-Mw(e) Closed Cycle Water Reactor Study, Vol. II, USAEC Report WCAP-2385, March 1963.
3. A. L. Gaines and L. Porse, Problems in the Design and Construction of Large Reactor Vessels, presented at the Third United Nations International Conference on the Peaceful Uses of Atomic Energy, Geneva, 1964, Paper A/Conf.28/P/227.
4. J. C. Rengel, Project Manager, Large Closed-Cycle Water Reactor Research and Development Program, Progress Report for the Period December 1, 1960 to May 31, 1961, USAEC Report WCAP-3703, Westinghouse Electric Corp., Atomic Power Division.
5. J. C. Rengel, Project Manager, Large Closed-Cycle Water Reactor Research and Development Program, Progress Report for the Period June 1, 1961 to August 31, 1961, USAEC Report WCAP-3706, Westinghouse Electric Corp., Atomic Power Division.
6. N. R. Nelson, Project Manager, Large Closed-Cycle Water Reactor Research and Development Program, Progress Report for the Period September 1, 1961 to November 30, 1961, USAEC Report WCAP-3707, Westinghouse Electric Corp., Atomic Power Division.
7. N. R. Nelson, Project Manager, Large Closed-Cycle Water Reactor Research and Development Program, Progress Report for the Period December 1, 1961 to February 28, 1962, USAEC Report WCAP-3708, Westinghouse Electric Corp., Atomic Power Division.
8. N. R. Nelson, Project Manager, Large Closed-Cycle Water Reactor Research and Development Program, March 1, 1962 to June 30, 1962, USAEC Report WCAP-3710, Westinghouse Electric Corp., Atomic Power Division.
9. Westinghouse Electric Corp., Atomic Power Division, 1962. (Unpublished)
10. Westinghouse Electric Corp., Atomic Power Division, 1962. (Unpublished)
11. Westinghouse Electric Corp., Atomic Power Division, 1963. (Unpublished)
12. Westinghouse Electric Corp., Atomic Power Division, 1963. (Unpublished)
13. Westinghouse Electric Corp., Atomic Power Division, 1963. (Unpublished)
14. Westinghouse Electric Corp., Atomic Power Division, 1963. (Unpublished)
15. C. Roderick, Project Manager, Large Closed-Cycle Water Reactor Research and Development Program, Progress Report, January 1, 1964 to March 31, 1964, USAEC Report WCAP-3269-2, Westinghouse Electric Corp., Atomic Power Division.
16. D. E. Byrnes and W. E. Foster, Literature Values for Selected Chemical/Physical Properties of Aqueous Boric Acid Solutions, USAEC Report WCAP-1570, Westinghouse Electric Corp., Atomic Power Division, January 1961.
17. W. D. Fletcher, A. Krieg, and P. Cohen, The Behavior of Austenitic Stainless Steel Corrosion Products in High Temperature Boric Acid Solutions, USAEC Report WCAP-1689 (Rev.), Westinghouse Electric Corp., Atomic Power Division, May 1961.
18. P. Cohen and G. R. Taylor, Ion-Exchange with Equilibrium and Decay, USAEC Report WCAP-1700, Westinghouse Electric Corp., Atomic Power Division, January 1961.
19. A. N. Nahavandi and G. B. Killinger, Primary System Pressure Response Study Due to Power Unbalance (TOPS Code), USAEC Report WCAP-1831, Westinghouse Electric Corp., Atomic Power Division, September 1961.
20. L. S. Tong, H. B. Currin, and A. G. Thorp II, New DNB (Burnout) Correlations, USAEC Report WCAP-1997 (Rev. 2), Westinghouse Electric Corp., Atomic Power Division, May 1963.
21. J. E. Olhoeft, The Doppler Effect for a Non-Uniform Temperature Distribution in Reactor Fuel Elements, USAEC Report WCAP-2048, Westinghouse Electric Corp., Atomic Power Division, July 1962.
22. A. S. Kitzes, Design and Hazards Report, LRD Irradiation Test Number 1, USAEC Report WCAP-3701, Westinghouse Electric Corp., Atomic Power Division, July 15, 1963.
23. W. Zernik, H. B. Currin, E. Elyash, and G. Previti, "THINC," A Thermal Hydrodynamic Interaction Code for a Semi-Open or Closed Channel Core, USAEC Report WCAP-3704, Westinghouse Electric Corp., Atomic Power Division, February 1962.
24. R. A. Dannels and Dermot J. Bredin, Compilation of a Muft Library (Library 567), USAEC Report WCAP-3709, Westinghouse Electric Corp., Atomic Power Division, December 1962.
25. W. J. Eich, H. T. Williams, Jr., and H. Aisu, The Heterogeneous Representation of Control Rods in Light Water Lattices: A Comparison of Analysis and Experiment, USAEC Report WCAP-3711,

Westinghouse Electric Corp., Atomic Power Division.

26. D. E. Byrnes, Some Physicochemical Studies of Boric Acid Solutions at High Temperatures, USAEC Report WCAP-3713, Westinghouse Electric Corp., Atomic Power Division, September 1962.
27. J. S. Moore, and B. H. Axelson, Reactor Control and Protection System Study for Chemical Shim Operation of a Large Closed Cycle Water Reactor, USAEC Report WCAP-3714, Westinghouse Electric Corp., Atomic Power Division, October 1962.
28. W. D. Fletcher, Ion Exchange in Boric Acid Solutions with Radioactive Decay, USAEC Report WCAP-3716, Westinghouse Electric Corp., Atomic Power Division, November 1962.
29. R. E. Wolf and J. F. Noonan, RENEWED: A Program for Nuclear Reactor Fuel Cycle Analysis, USAEC Report WCAP-3717, Westinghouse Electric Corp., Atomic Power Division, November 1962.
30. D. L. Miller, Control Rod Programming in a Large Multiregion Core, USAEC Report WCAP-3719, Westinghouse Electric Corp., Atomic Power Division, October 1962.
31. P. G. Lacey, Reactivity Dependence Upon Moderator Temperature and Boron Concentration in Large PWR Cores Controlled by Chemical Shim, USAEC Report WCAP-3720, Westinghouse Electric Corp., Atomic Power Division, November 1962.
32. A. N. Nahavandi, B. H. Axelson, G. B. Killinger, and A. H. Killinger, A Digital Computer Analysis of Closed Cycle Water Nuclear Power Plant Start-Up Using Natural Circulation (THERMO-SYPHON Code) Vols. I and II, USAEC Report WCAP-3722, Westinghouse Electric Corp., Atomic Power Division, February 1962.
33. P. G. Lacey, Fine Structure Power Peaking in a Critical Experiment Mockup of a Chemical Shim Core, USAEC Report WCAP-3723, Westinghouse Electric Corp., Atomic Power Division, March 1963.
34. H. Aisu, R. F. Barry, and P. G. Lacey, Load Variation Restrictions in a Chemically Poisoned Large PWR Core, USAEC Report WCAP-3724, Westinghouse Electric Corp., Atomic Power Division, March 1963.
35. D. L. Miller, Control Rod Requirements in a Chemical Shim Core, USAEC Report WCAP-3727, Westinghouse Electric Corp., Atomic Power Division, August 1963.
36. L. F. Picone, The In-Pile Test of Chemical Shim, USAEC Report WCAP-3729, Westinghouse Electric Corp., Atomic Power Division, June 1963.
37. L. F. Picone, D. D. Whyte, and G. R. Taylor, Radiotracer Studies of Hideout at High Temperature and Pressure, USAEC Report WCAP-3731, Westinghouse Electric Corp., Atomic Power Division, June 1963.
38. L. E. Strawbridge and R. E. Wolf, Optimization Study for Large Pressurized Water Reactor Cores, USAEC Report WCAP-3733, Westinghouse Electric Corp., Atomic Power Division, Apr. 8, 1964.
39. R. A. Dean, Coolant Mixing in Open Lattice Reactor Cores, USAEC Report WCAP-3735, Westinghouse Electric Corp., Atomic Power Division, August 1963.
40. EBWR Project Group, EBWR Test Reports (100-MWT Operation), USAEC Report ANL-6703, Argonne National Laboratory, January 1964.
41. Allis-Chalmers Mfg. Co., Atomic Power Development Associates, Inc., and The Babcock & Wilcox Co., Large Fast Reactor Design Study, USAEC Report ACNP-64503, January 1964.
42. Combustion Engineering, Inc., Liquid Metal Fast Breeder Reactor Design Study, USAEC Report CEND-200, Vols. I and II, January 1964.
43. General Electric Company, Atomic Power Equipment Department, Liquid Metal Fast Breeder Reactor Design Study, USAEC Report GEAP-4418, Vols. I and II, January 1964.
44. R. B. Steck (Comp.), Liquid Metal Fast Breeder Reactor Design Study, USAEC Report WCAP-3251-1, Westinghouse Electric Corp., Atomic Power Division, January 1964.
45. David Okrent, Neutron Physics Considerations in Large Fast Reactors, *Power Reactor Technol.*, 7(2): 107-137 (Spring 1964).
46. Chicago Operations Office, Reactor Engineering Division, An Evaluation of Four Design Studies of a 1000-MWe Ceramic-Fueled Fast Breeder Reactor, USAEC Report COO-279, Dec. 1, 1964.
47. L. J. Koch, F. S. Kirn, G. W. Wensch, C. E. Branyan, and E. L. Alexanderson, Sodium Cooled Fast Breeder Reactors, presented at the Third United Nations International Conference on the Peaceful Uses of Atomic Energy, Geneva, 1964, Paper A/Conf.28/P/207.
48. David Okrent, K. P. Cohen, and W. B. Loewenstein, Some Nuclear and Safety Considerations in the Design of Large Fast Power Reactors, presented at the Third United Nations International Conference on the Peaceful Uses of Atomic Energy, Geneva, 1964, Paper A/Conf.28/P/267.
49. Leonard E. Link, George J. Fischer, and Edwin L. Zebroski, Fuel Cycle Economics of Fast Reactors, presented at the Third United Nations International Conference on the Peaceful Uses of Atomic Energy, Geneva, 1964, Paper A/Conf.28/P/248.
50. C. E. Klotz and R. S. Miller, The Design of a 1000 MWe Fast Breeder Reactor, *Trans. Am. Nucl. Soc.*, 7(1): 196 (June 1964).
51. L. S. Noderer and Sidney Visner, Effect of a Voided Gap on Reactivity Coefficient for Voiding Core Sodium in a Fast Reactor, *Trans. Am. Nucl. Soc.*, 7(2): 238 (November 1964).

NUCLEAR SCIENCE ABSTRACTS

The U. S. Atomic Energy Commission, Division of Technical Information, publishes *Nuclear Science Abstracts (NSA)*, a semimonthly journal containing abstracts of the literature of nuclear science and engineering.

NSA covers (1) research reports of the U. S. Atomic Energy Commission and its contractors; (2) research reports of government agencies, universities, and industrial research organizations on a world-wide basis; and (3) translations, patents, books, and articles appearing in technical and scientific journals.

Complete indexes covering subject, author, source, and report number are included in each issue. These are cumulated quarterly, semiannually, and annually providing a detailed and convenient key to the literature.

Availability of *NSA*

SALE *NSA* is available on subscription from the Superintendent of Documents, U. S. Government Printing Office, Washington, D. C., 20402, at $30.00 per year for the semimonthly abstract issues and $22.00 per year for the four cumulated-index issues. Subscriptions are postpaid within the United States, Canada, Mexico, and all Central and South American countries, except Argentina, Brazil, British and French Guiana, Surinam, and British Honduras. Subscribers in these Central and South American countries, and in all other countries throughout the world, should remit $37.00 per year for subscriptions to semimonthly abstract issues and $25.00 per year for the four cumulated-index issues.

EXCHANGE *NSA* is also available on an exchange basis to universities, research institutions, industrial firms, and publishers of scientific information. Inquiries should be directed to the Division of Technical Information Extension, U. S. Atomic Energy Commission, P. O. Box 62, Oak Ridge, Tennessee, 37831.

TECHNICAL PROGRESS REVIEWS may be purchased from Superintendent of Documents, U. S. Government Printing Office, Washington, D. C., 20402. *Isotopes and Radiation Technology* at $2.00 per year for each subscription or $0.55 per issue; the other four journals at $2.50 per year and $0.70 per issue. The use of the coupon below will facilitate the handling of your order.

POSTAGE AND REMITTANCE: Postpaid within the United States, Canada, Mexico, and all Central and South American countries except as hereinafter noted. Add $0.50 per year, or $0.15 per single issue for the *Isotopes and Radiation Technology* journal and $0.75 per year or $0.20 per single issue for the other four journals for postage to all other countries, including Argentina, Brazil, British and French Guiana, Surinam, and British Honduras. Payment should be by check, money order, or document coupons, and MUST accompany order. Remittances from foreign countries should be made by international money order, or draft on an American bank, payable to the Superintendent of Documents, or by UNESCO book coupons.

order form

SUPERINTENDENT OF DOCUMENTS
U. S. GOVERNMENT PRINTING OFFICE
WASHINGTON , D. C., 20402

Enclosed:
document coupons ☐ check ☐ money order ☐

Charge to Superintendent of Documents No. _____

Please send a one-year subscription to

☐ NUCLEAR SAFETY

☐ POWER REACTOR TECHNOLOGY

☐ REACTOR FUEL PROCESSING

☐ REACTOR MATERIALS

(Each subscription $2.50 per year; $0.70 per issue.)

☐ ISOTOPES AND RADIATION TECHNOLOGY

(Each subscription $2.00 a year; $0.55 per issue.)

SUPERINTENDENT OF DOCUMENTS
U. S. GOVERNMENT PRINTING OFFICE
WASHINGTON, D. C., 20402

(Print clearly)

Name _____

Street _____

City _____ Zone ____ State _____